Chapter 2
Advances in Spectro-Polarimetric Light-Scattering by Particulate Media

Romain Ceolato and Nicolas Riviere

2.1 Introduction

Electromagnetic light-scattering refers to the general physical process where electromagnetic radiations do not follow trajectories predicted by the law of reflection. This phenomenon is a general term used to describe the light scattered by a surface, a single particle, as well as complex systems of particles. Particulate media are systems of randomly positioned particles with arbitrary shapes in absorbing or non-absorbing host-media. The light scattered by such media produces distinct signatures or fingerprints, which may depend on wavelength, polarization, time-propagation, and directions. These signatures have been a growing interest for characterization of particulate media in different scientific and industrial fields. The purpose of this chapter is to provide insights into spectro-polarimetric light-scattering by particulate media. It also sets out to demonstrate the place of spectro-polarimetric light-scattering as a robust and comprehensive optical diagnostic method for particulate media composed of small particles found in several fields of science and engineering.

In atmospheric science, meteorology, and remote-sensing, particulate media refers to aerosols (e.g. dust, sand, spores, or sea salts) or hydrometeors (e.g. clouds, fog, rain). These particles are classified as either natural (i.e. produced by nature) or anthropogenic aerosols (i.e. produced from human activities). Much attention has been given lately on fine and ultrafine anthropogenic aerosols such as soot and sulfate particles as they present a severe respiratory health hazard in urban environments. High concentrations of airborne pollutants in the atmosphere result in substantial

R. Ceolato (✉) · N. Riviere
Optronics Department, ONERA, The French Aerospace Lab,
31055 Toulouse, France
e-mail: Romain.Ceolato@onera.fr

N. Riviere
e-mail: Nicolas.Riviere@onera.fr

A. Kokhanovsky (ed.), *Springer Series in Light Scattering*, Springer Series
in Light Scattering, https://doi.org/10.1007/978-3-319-70808-9_2

radiative perturbations which impact the energy transfer between the sun and earth-ground: this phenomenon is referred as radiative forcing and plays a significant role in climate change. Soot particles are the second most important human emissions concerning climate-forcing, and only carbon dioxide is estimated to have a greater effect (Bond et al. 2013). The study of particulate media is also of great interest in diverse fields such as combustion science for public health monitoring (e.g. combustion particles from diesel engines) or defense and security (e.g. combustion particles from aircraft engines, plumes, rockets, or jets). Various processes produce particulate media in numerous industrial products. For instance, nanoparticles produced by different techniques (e.g. milling, attrition, and nucleation) which attract much attention today because of their unique chemical and physical properties. In biomedical research, particulate media in liquids are found in several living organisms (e.g. cells, nuclei, or bacteria). Bio-aerosols are another important issue for public health as these aerosols may present serious threats for societies (e.g. biological warfare agents). Finally, in astrophysics and cosmology, the study of regolith or cosmic and interplanetary dust is of particular importance in understanding phenomena such as star or solar system formations (Pilbratt et al. 2010).

A wide variety of techniques is available to characterize particulate media. Optical techniques are good candidates for probing particulate media with particles size close to the radiation wavelength because particles effectively scatter light with wavelengths close to their size. The first category of techniques implies sampling and collecting the particles for physicochemical analysis. These methods are often used in chemical or industrial engineering for their relative simplicity although sampling of particles may modify the characteristics of the particles. A second category refers to remote probing technique. They require higher technicity and sophisticated analysis to extract relevant information about the particles but can be undertaken in-line without causing any disturbance of the media. Light-scattering techniques belong to both categories as they can characterize statistically significant numbers of particles simultaneously. They provide valuable information such as particle size distributions, morphology, concentration, internal structure, or relative complex refractive index. Depending on the applications or particles of interest, different terrestrial, remote (i.e. airborne, space) or laboratory instruments measure light-scattering data to probe particulate media. Well known LIDAR (LIght Detection And Ranging) techniques, the optical counterpart of microwave RADAR (RAdio Detection And Ranging), are used to remotely profile aerosols in the atmosphere spanning from the ultraviolet (UV) to the infrared (IR) spectrum with polarization analysis. They provide long-range aerosol profiles and associated inverse methods allow the retrieval of different microphysical properties. For laboratory analysis, SLS (Static Light-Scattering) or DLS (Dynamic Light-Scattering) are other well-established light-scattering techniques used to probe small particles. Light-scattering remains a complex problem though it provides precious information on an extensive range of particles such as aerosols, blood cells, or colloidal suspensions. As an example, the light scattered by particulate media is governed by the microphysical parameters of the particles, including the size, the shape, and the complex refractive index. However, this dependence is complex, and measurements cannot directly retrieve these physical parameters due to the non-unique solution of the solved problem. Light-scattering can be considered as a direct and an inverse light-scattering problem. Solving the direct problem implies computing the scattered radiation for a given particulate medium and illumination. Solving the inverse problem means to retrieve the properties of a particulate medium from the scattered radiation for a given illumination. In practice, inversion methods for light-scattering have been developed to retrieve the microphysical properties of particles from light-scattering measurements. Errors often marred these methods (e.g. errors on initial parameters, invalid assumptions). Several challenges related to the inverse light-scattering problem are given below:

The non-unique solution. A first major challenge comes from the existence of singularities in the inverse scattering problem, i.e. identical light-scattering patterns can be obtained from different microphysical parameters. This problem is usually referred as the non-uniqueness problem of light-scattering. The inverse light-scattering problem is not a *well-posed* problem in the sense of Hadamard (1902) and is termed as an *ill-posed* problem. Most of these inversion methods are conditioned to prior knowledge about the particulate media of interest. For instance, particle size can be retrieved from angular data as long as the refractive index is known. The morphology or relative complex refractive index of the particles is most of the time assumed or known a priori to retrieve the Particle Size Distribution (PSD) of particulate media from light-scattering measurements (e.g. LIDAR or SLS/DLS measurements and their associated inverse techniques). In cases where the relative complex refractive index is unknown or when it changes upon experimental conditions (e.g. heating or chemical processes), severe uncertainties result in the sizing of the particles. In such cases, one can determine the relative complex refractive index as long as PSD is provided by external instruments such as aerosol impactors or particles counter (Gramm et al. 1974a, b) which may result in uncertainties.

The single-scattering assumption. A second challenge comes from the use of unsuitable and unverified physical assumptions. Many light-scattering inverse methods are based on the single-scattering approximation, especially in the field of LIDAR (Klett 1981). They assume that light is scattered only once by particles before detection. This assumption is suitable and gives good results for particulate media with a low concentration or a small optical path (e.g. weak aerosol plumes, diluted colloidal solutions). For instance, the inversion of LIDAR measurements is based on the single-scattering LIDAR equation to retrieve aerosol PSD or optical coefficients (Scheffold and Cerbino 2007). This operation could change the chemical properties of the media and may result in additional uncertainties on the value of the concentration. Multiple-scattering is most of the time ignore while it occurs for intermediate and highly concentrated particulate media. Knowing whether particulate media are dense, or non-dense is hard to define as it depends on the particulate medium itself (e.g. size, concentration, optical index) but also on the wavelength of light: a given particulate medium can be regarded as dense in the UV spectrum while can be considered non-dense in the far-IR spectrum. In other words, the single-scattering approximation has to be used with a great care before inverting light-scattering data.

Limited information. A third challenge comes from experimental limitations. Light-scattering by particulate media depends on all the properties of the incident light: angular (or directional) distribution, polarimetric state, wavelength, and even time for pulsed light sources. Most experimental instruments are not able to measure all these modifications at the same time. They must be restricted to limited angles, polarimetric states, or wavelengths (e.g. single wavelength LIDAR, unpolarized SLS). Such limitations restrict by nature the capacity of light-scattering based instruments.

Experimental errors. Besides, statistical errors may induce incapacity to measure light-scattering for a given particulate medium accurately. The solution of the scattering problem is highly sensitive to errors in measurements and calculated scattering properties.

Light-scattering signatures often result in large amounts of information, and because analytical inversion is not always feasible because of the above challenges, the retrieval of microphysical parameters is a complex task. One option to relax these difficulties is to fuse spectral and polarimetric properties of scattered light. The merge of spectral, polarimetric, and multi-angle information about light-scattering is proposed as a comprehensive tool to characterize particulate media by relaxing different assumptions about the media. Recently, a growing amount of interest has been raising in spectro-polarimetric light-scattering in several fields from remote-sensing to wider applications such as astrophysics (Kimura et al. 2003), biomedical (Ghosh et al. 2011; Patskovsky et al. 2014), active (Manninen et al. 2014) and passive remote-sensing (Powers and Davis 2012; Diner et al. 2013; Zieger et al. 2007), particle analysis (Tang and Lin 2013; Sharma et al. 2013; Bendoula et al. 2015), defense, and security (Lambert-Girard et al. 2012). Spectro-polarimetric light-scattering techniques are expected to improve the understanding of scattering phenomena and identification of relevant microphysical parameters of complex particulate media. Although numerous topics involve spectral and polarimetric light-scattering, including spectral or polarimetric laser imaging systems (Powers 2012), or spectro-polarimetric imaging systems (Diner et al. 2013), these questions fall out of the scope of this review. We restrict the analysis to the characterization of particulate media by spectro-polarimetric light-scattering.

The recent advances of spectral and polarimetric light-scattering by particulate media, including single and multiple scattering, are reviewed as follow: (i) a brief introduction to light-scattering by particulate media, (ii) a state-of-the-art of the different existing spectral—from multi-spectral to hyperspectral—light-scattering methods, (iii) a state-of-the-art of the different polarimetric light-scattering methods, and (iv) a comprehensive review of the recent advances and contributions of the merging of spectro-polarimetric information for light-scattering, including radiative transfer simulations and measurements carried out at ONERA, The French Aerospace Lab.

2.2 Problem of Light-Scattering by Particulate Media

The interaction between particles and incident electromagnetic waves produces oscillations of electric charges, which results in scattering and absorption. Particulate media are defined as heterogeneous media composed of particles (e.g. aerosols, colloids) within a host medium (e.g. air, water). Such media can be termed as non-dense or dense particulate media, depending on the volume concentration of particles. Light-scattering by particulate media depends on (i) the size, (ii) the shape, and (iii) the complex refractive index $m = n - i \cdot k$ of the particles where n is the real refractive index and k the absorption coefficient. The index m refers to the relative index between the particle and host media (e.g. air or water).

The problem of light-scattering by a random distribution of particles has found broad interest in different scientific fields such as atmospheric science, particle characterization, biomedical and remote-sensing, specially studied in the LIDAR community. This section reviews the general principle of light-scattering in regard with the single scattering (i.e. when the number of scattering events is equal to unity) and multiple scattering approximations (i.e. when the number of scattering events is higher than unity).

2.2.1 *Single Light-Scattering*

Single light-scattering refers to the scattering of electromagnetic waves by a single particle. This approximation remains valid for non-dense or weak particulate media with low particles concentrations such as dispersed aerosols in the atmosphere. For such media, as represented in Fig. 2.1, a single scattering event occurs between the emission and detection of light.

Light-scattering by a single particle has been an object of interest for more than a century from the historical Lorenz works (Lorenz 1890), who solved the scattering problem for transparent spheres, and Mie works (Mie 1908) who published a complete theory describing the interactions between an electromagnetic wave and a homogeneous spherical metallic particle. The Lorenz-Mie theory provides solutions

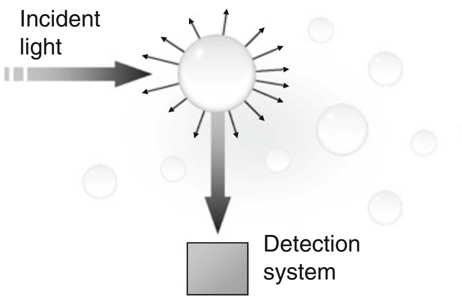

Fig. 2.1 Representation of single light-scattering

of the scattering problem for colloidal suspensions in the form of an infinite series of vector spherical harmonic expansion, which satisfies Maxwell's equations (Maxwell 1865). From Lorentz-Mie solutions, several radiative parameters such as efficiency, cross-sections, or differential cross-sections relative to scattering, absorption, and extinction are derived. The solutions of the Lorenz-Mie theory are directly related to two physical parameters:

(1) the *relative complex refractive index* $m = n/n_h$ where $n = n_p - ik_p$ is the complex refractive index of the particle and n_h is the real refractive index of the host medium,
(2) and the *size-wavelength parameter* x defined as $x = 2 \cdot \pi \cdot r/\lambda$ where r is the radius of the spherical particle and λ the considered wavelength (Bohren and Huffman 1998).

This parameter was used by Lord Rayleigh (Young 1981) to define light-scattering by small particles compared to the wavelength and was later used by Van de Hulst (1981) to categorize light-scattering into different *light-scattering regimes*. Light-phase variations, which are induced when light passes through a particle and defined by $\delta = 2m \cdot x$, govern these light-scattering regimes. All the various scattering regimes are reported in a $m - x$ diagram similar to the one given in Fig. 2.2 where the x ranges from zero for ultrafine particles to infinity for large particles and, m ranges from zero for optically soft particles to infinity for optically hard particles.

For a small relative complex refractive index, the scattering regimes are either Rayleigh-Debye-Gans regime (region 1) for large or intermediate size parameter, or anomalous diffraction regime (region 2) for small size parameters. Rayleigh regime (region 6) applies for small size parameters with intermediate relative refractive index, and geometrical optics regime (region 3) applies for large size parameters with intermediate relative index. For a large relative refractive index, the scattering regimes are either total reflection regime (region 4), for a large or intermediate size parameter, or optical resonance regime (region 5) for a small size parameter. Mie regime (central region) applies for intermediate size parameters or particle sizes comparable to the wavelength and intermediate relative refractive index, and no

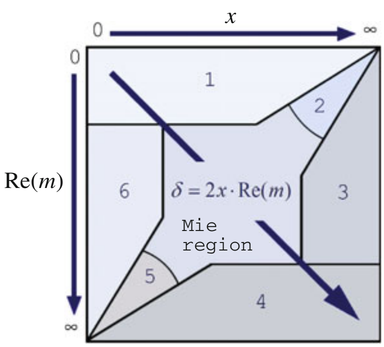

Fig. 2.2 Light-scattering regimes categorized in the x-m diagram. Region 1: Rayleigh-Debye-Gans regime. Region 2: Anomalous diffraction regime. Region 3: Geometrical optics regime. Region 4: Total reflection regime. Region 5: Optical resonance regime. Region 6: Rayleigh regime

approximation can be made as light-phase shifts cannot be neglected. Further comprehensive discussions on light-scattering regimes can be found in Van de Hulst works (Van de Hulst 1981; Mishchenko et al. 2002).

Regularly-shaped particles, such as spheres, follow the Lorenz-Mie theory. The theory remains valid with no size limitation as the solutions converge to the limit of geometric optics for large particles as well as to the limit of the Rayleigh theory for very small particles including molecules. This theory has been later extended to a more general theory named Generalized Separation of Variable (GSV) method to take into account different regularly-shaped particles different from spheres such as homogeneous spheroidal particles (Asano 1976; Gouesbet 2011). Problems involving complex regularly-shaped particles with large varieties of geometries (axisymmetric, non-axisymmetric, composite or layered and inhomogeneous) (Doicu and Wriedt 1999) have used extensively another category of methods known as the Surface-Integral Equation (SIE). Different numerical implementations of these methods are available, such as the superposition T-matrix (Mackowski 1996; Mishchenko et al. 2000; Liu et al. 2008). One advantage of these methods is their short computation time, though they remain limited to regularly-shaped particles with a specific range of size parameters. In addition, one must avoid using these methods to compute the radiative properties of particles with high-aspect ratios as the problem becomes ill-conditioned for very large objects compared with a wavelength. We refer to the work of Mishchenko et al. (2002) for a detailed review of the advantages and constraints of the different light-scattering numerical methods.

Irregularly-shaped or realistic particles usually do not present regularly-shaped geometries. The simplistic concept of *equivalent-volume or equivalent-surface* sphere is commonly used to compute light-scattering properties of particles without taking into account shape effects (Kalashnikova and Sokolik 2004). Several investigations have shown that most of these particles have non-spherical geometries (Okada et al. 2001; Munoz and Hovenier 2011) and that optical properties may vary considerably depending on their shape (Yang et al. 2007; Yi et al. 2011). However, for the sake of simplicity, most studies assumed that particles have a spherical or spheroidal geometry despite the fact that the majority of particles found in nature (e.g. dust, ashes) are not regularly-shaped. Accurate computation of light-scattering properties of irregularly-shaped particles requires the use of more complex and time expensive methods. Another category of methods based on the Volume-Integral Equation (VIE) provide solutions which fully account the particles geometry since the Lorenz-Mie and SIE methods do not directly apply to irregularly-shaped particles. These methods compute light-scattering by particles by discretization of the particle into a distribution of discrete dipoles regarding the morphology of the particle. Dipole-dipole couplings model the interactions between dipoles (Markel et al. 1991). The total electric field is considered as an incident electric field and a superposition of all the electric field from all the surrounding dipoles. Implementations are used depending on the discretization techniques such as the Discrete Dipole Approximation (DDA) proposed by Purcell and Pennypacker (1973). With increasing dipole number, these methods can be time-consuming and singular kernel problems may rise. In spite of these limitations, these methods remain traditional to compute light-scattering properties of irregularly-shaped particles thanks to their flexibility and physical approach (Draine and Flatau 1994). Other electromagnetic scattering methods address the problem of electromagnetic scattering by irregularly-shaped particles. For instance, the Finite Difference Time Domain (FDTD) methods are widely used in the field of RADAR (Yee 1966; Tang and Aydin 1995) in order to solve complex scattering problems, such as electromagnetic scattering by rough surfaces (Hastings and Schneider 1995; Sun et al. 2013a, b, c), or scattering by arbitrary shaped and inhomogeneous particles (Yang and Liou 1996; Yang et al. 2000; Sun et al. 2009, 2011). Either DDA or FDTD techniques present different advantages and drawbacks concerning applications and performances.

2.2.2 Multiple Light-Scattering

Particulate media are composed of multiple particles for intermediate or high concentration that the single-scattering approximation does not hold. For particulate media such as clouds, dense plumes, jets, or foams, multiple scattering events may occur between the emission and detection of light. Thus, the widely used single-scattering approximation is no longer valid (Ishimaru et al. 1984) (Fig. 2.3).

The Radiative Transfer Theory (RTT), which originates from Lommel (1889) and Chwolson (1889) independent works, models the propagation of electromagnetic waves in particulate media with multiple scattering. Schuster (1905) introduced the two-stream Radiative Transfer Equation (RTE) which provides analytical solutions to a single layer plane-parallel radiative transfer equation. Using the

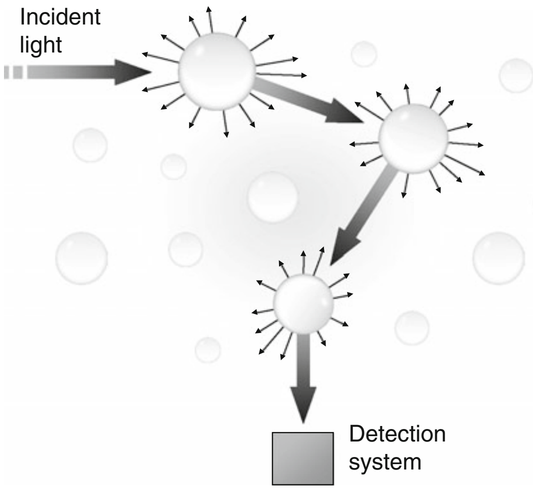

Fig. 2.3 Representation of multiple light-scattering

invariance principle, Ambartsumian (1943, 1947) proposed a simple solution of the RTE to solve the problem of diffuse reflection of light by a scattering medium, and Chandrasekhar (1950) solved the problem for a finite isotropic scattering medium using the discrete ordinate method. This method models the particulate medium as a semi-infinite plane–parallel multi-layered isotropic scattering medium to account multiple-scattering. This theory was later extended with great results for several applications in astrophysics, remote-sensing, biomedical and other scientific areas, including anisotropic particulate media (Ishimaru et al. 1984). Traditionally, the RTE is considered as a phenomenological equation based on heuristic principles of classical radiometry; yet it was derived from first-principles and Maxwell's equations using statistical electromagnetics (Mishchenko 2011). However, no electromagnetic coherence effects are modeled and taken into account since the RTE is only based on light intensity flux transfers. It restricts the use and validity of this approach to particulate media with moderate particle concentration, i.e. where the distance between particles is larger than the wavelength. One essential condition for validity is that the scattering events should always occur in the far-field region of each particle in order to prevent the apparition of short-range inter-particle correlations effects such as dependent scattering (e.g. aggregates, closely-packed particles). This is sometimes referred as the *independent multiple-scattering approximation*.

In the following section, an overview of spectral light-scattering by particulate media is presented for a broad range of applications. The advantages of studying light-scattering properties at different wavelengths or frequencies are highlighted as well as the associated challenges for optical diagnostic using this method.

2.3 Spectral Light-Scattering

Wavelength, or frequency, is a fundamental property of electromagnetic waves. Standard light-scattering methods have studied the propagation of monochromatic plane waves through particulate media. Radiative parameters such as extinction, scattering, and absorption coefficients, often present distinct wavelength dependencies due to different physical phenomena (Van de Hulst 1981). The scope of this section is to present a non-exhaustive state-of-the-art of spectral light-scattering methods. Techniques with single wavelength capabilities are not considered in this section. Though several methods measure broadband electromagnetic scattering properties in the microwave and terahertz region, these are out of the scope of this review as the spectral domain of interest is limited to methods which cover wide spectral domain in the UV, visible, and IR wavelengths.

Light-scattering by spherical particles, according to Lorenz-Mie theory, exhibits resonances which depend upon the values of size parameter x and relative complex refractive index m. Single-wavelength light-scattering methods can address a single light-scattering regime in the $m-x$ diagram presented in Fig. 2.2. However, for a given single and fixed-wavelength, the scattered intensity shows dependencies on both particle size and relative refractive index. This non-uniqueness problem has raised a fundamental limitation of single-wavelength light-scattering methods: equivalent light-scattering signatures can be obtained either by changing the particles size or by varying the particles relative refractive index. Therefore, the inference of the microphysical properties based only on single-wavelength light-scattering measurements has led to highly questionable results, unless additional information was known a priori (Janzen 1979). In the absence of such additional information, the uniqueness of particle size and relative refractive index inferred by single-wavelength light-scattering methods cannot be assured.

Spectral or multi-wavelength methods have been proposed (Ceolato 2016) to overcome the non-uniqueness problem of light-scattering and to infer microphysical properties with no a priori knowledge of the media. The objective of these spectral methods is to address a full series of light-scattering regimes in the $m - x$ diagram by analyzing light-scattering over a broad spectrum. For non-dispersive particulate media, i.e. m does not depend on the wavelength; m is invariant for a series of x values: the $m - x$ series describes a straight line in the diagram, perpendicularly to the m-axis. For dispersive particulate media, i.e. m depends on the wavelength; m varies for a series of x values: the $m - x$ series describes a curved line in the diagram, where the curvature of is directly related to the variation of the relative complex refractive index. Thanks to this simple idea, methods based on spectral light-scattering intensities are proposed for unambiguous inference of microphysical properties of particulate media.

In astrophysics research, spectral light-scattering measurements were first carried out to study particulate planetary surfaces. Also known as color-ratio imaging, these techniques have been effective ways to study the chemical and mineral composition of the Moon for instance (McCord 1969; McCord et al. 1972; Pieters 1999). Because the illuminating/observing geometry plays a secondary role in the spectral reflectance of planetary surfaces, multi-spectral measurements at different phase angles were first compared, without accounting the polarization effects, to provide valuable information on the lunar surface composition (McCord 1969). In the field of remote-sensing and atmospheric studies, sensing and detecting of atmospheric particulate matter (e.g. biomass burning particles, soot particles, sea salts) have used light-scattering to retrieve microphysical properties of interest (Holben et al. 1998). Among them, spectral light-scattering techniques remain a vast area of research to remotely sense and detect particles and are usually classified into two categories: passive and active optical techniques. Both techniques have proved to be convenient to monitor atmospheric aerosols and to evaluate their impact on climate. Both methods present certain advantages and deficiencies (Deirmendjian 1980).

Total (or angularly integrated) spectral light-scattering measurements, such as extinction measurements, have always been experimentally much simpler than multi-directional or angularly resolved light-scattering. Nevertheless, the inverse problem associated with extinction present no unique solution for a single wavelength: a measured extinction coefficient may correspond to any combination of particle size and relative complex refractive index (Janzen 1979). Ångström first suggested in 1929 an empirical relationship between the particle size and the wavelength dependence of the extinction coefficient (or optical depth) of light by aerosols. A spectral relation between the atmospheric visibility (defined from the extinction coefficient) and backscattering coefficient was later proposed the 1950s based on long-range atmospheric transmission measurements (Curcio and Knestrick 1958). The advantage of broadband over monochromatic light sources has been theoretically demonstrated to infer aerosols particle size distribution from the spectral extinction-to-backscatter ratio (Twomey and Howell 1965; Foitzik 1965). First numerical inversion based on spectral extinction coefficient measurements was performed by Yamamoto (1969) to retrieve the particle size distribution. Other methods were later deployed to determine number-size distributions of particulate media composed of regularly (Yamamoto and Tanaka 1969; Box and McKellar 1978; Nilsson 1979; Klett 1984) and irregularly-shaped (Liu et al. 1999; Tang 2013) particles. For instance, spectral extinction measurements, from broadband light-source in the visible and infrared, coupled with Lorenz-Mie theory based inversion methods were developed to probe various hydrometeors such as fog and haze (Lenham and Clay 1982). Several techniques have been developed to improve numerical inversion (Grassl 1971; Shaw et al. 1973a, b; King et al. 1978). Among them, the constraint imposed by the Kramers-Kronig relation (Landau and Lifshitz 1960) has been proposed to determine the real and complex part of the relative complex refractive index of particles, including aerosols (Milham et al. 1981), water clouds, and hazes (Deirmendjian 1964).

Angular (or angularly resolved) spectral light-scattering methods have been developed to probe particulate media from multi-spectral nephelometry to diffuse light-scattering, most of the time in weak multiple scattering regimes. Different remote-sensing techniques use a natural light source (e.g. Sun or Moon) to perform spectral light-scattering measurements. Such measurements are carried out to determine aerosol spectral properties of particulate media in polluted, haze, or cloudless days (Olsen et al. 1983; Vasilyev et al. 1995). Numerous instruments have been developed to measure optical properties of airborne particles from commercially available such as sky-photometers or albedometers, which measure the ratio of scattering to extinction or Single Scatter Albedo (SSA) (Dial et al. 2010). Spectral dependency of optical thickness was reported for different particles from desert dust, soot, or biomass burning (Vasilyev et al. 1995; Bergstrom et al. 2007). The retrieval of aerosol size distribution can be performed from spectral optical depth (Shaw et al. 1973a, b; Moorthy et al. 1991), whereas the retrieval of other aerosol parameters such as the complex refractive index cannot usually be performed without prior knowledge (Yang and Wenig 2009). Other remote-sensing techniques use an artificial light source (e.g. lamp or laser) to perform spectral light-scattering measurements. Spectral nephelometry consists in measuring the spectral light-scattering at multiple angles to investigate complex and dense particulate media (Elias and Cotte 2008). For instance, the relative complex refractive index of polystyrene microspheres was inferred from spectral light-scattering measurements (Ma et al. 2003). New techniques in nephelometry have been investigated using a SuperContinuum (SC) laser source with a series of filters

(Sharma et al. 2013), or highly sensitive techniques based on Cavity Ring-Down (CRD) spectroscopy (Lang-Yona et al. 2009; Zhao et al. 2014).

Range-resolved light-scattering techniques were developed to fill the gaps in the particle characterization. These active techniques use either incoherent or coherent artificial light sources (e.g. laser) and are important parts of atmospheric research. In optics, these techniques follow the principle of RADAR and are referred as LIDAR. First LIDAR systems employed incoherent continuous lamp to sense the molecular and aerosol composition of the atmosphere (Johnson et al. 1939; Bureau 1946). From the 1960s, with the development of the laser, several systems have integrated these new coherent light sources to become useful tools for measuring the vertical profiles of the aerosol optical properties. A series of laser pulses propagate through the atmosphere, and a sensor detects a small amount of backscattered light. The extent and properties of particulate media in the atmosphere can be retrieved from the magnitude of the backscattered light. In principle, the use of multi-wavelength or spectral LIDAR allows one to investigate the different ranges of particle size distribution of aerosols, which is due to the dependence of scattering properties on the wavelength of incident light. Relying on significant advances in novel laser sources, the concept of spectral LIDAR has gained notoriety based on the differential light-scattering and absorption over a spectral domain of interest (Fig. 2.4).

The first option for spectral LIDAR is to use different laser sources which emit a limited number of wavelengths to probe the atmosphere. Early works showed the feasibility of inferring additional information on the particulate media using simultaneous multi-wavelength LIDAR measurements (Heintzenberg et al. 1981; Feingold and Grund 1994). Wood (1984) theoretically studied backscattering coefficient as a function of wavelength, measurable by a multi-wavelength LIDAR, to identify the chemical composition of atmospheric aerosols. Muller and Quenzel (1985) numerically investigated the feasibility of determining the PSD from aerosol backscattering and extinction coefficients at four LIDAR wavelengths using a randomized minimization search technique. They found that accurately determined backscatter and extinction coefficients at four wavelengths carry enough information for a relatively good retrieval of the PSD, if the relative complex refractive index is known a priori. Qing et al. (1989) evaluated the feasibility of deriving PSD from extinction and backscattering coefficients measurements with a multi-wavelength LIDAR and proposed a regularization method assuming that

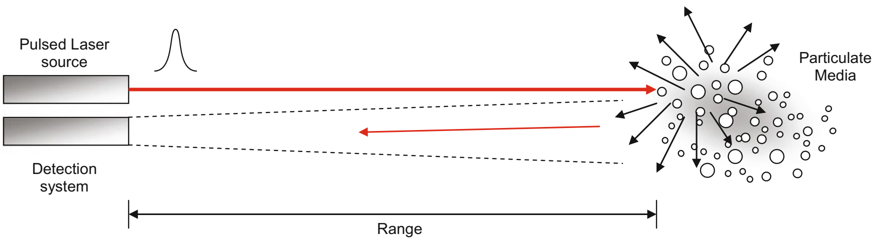

Fig. 2.4 General principle of a LIDAR system

these coefficients can be accurately measured from the LIDAR data. Sasano and Browell (1989) demonstrated the potential of a multi-wavelength LIDAR for discriminating the different aerosol types, such as maritime, continental, stratospheric, and desert, from the wavelength dependence of the aerosol backscattering coefficient. LIDAR In-space Technology Experiment (LITE) was the first LIDAR system sent into space to demonstrate and explore the capabilities of space LIDAR for atmospheric research (Couch et al. 1991). In addition to being a pioneer spaceborne LIDAR, LITE used three-wavelength laser sources to perform multi-spectral backscatter LIDAR measurements. Post et al. (1992) at NOAA observed ejecta from the eruption of Mt. Pinatubo at three wavelengths from visible to infrared. Del Guasta et al. (1994) fitted the multi-wavelength LIDAR data to a monomodal log-normal PSD and retrieved its associated mode radius. Based on multi-directional or of angularly dependent light intensity measurements, Yoshiyama et al. (1996) estimated PSD from bistatic multi-wavelength LIDAR measurements using 5–8 wavelengths. Rajeev and Parameswaran (1998) developed inversion methods dedicated to retrieving aerosols from dual-wavelength to multi-wavelength LIDAR measurements without any assumption on the form of the size distribution. Ligon et al. (2000) examined the feasibility of using a generalized stochastic inversion methodology to estimate PSD from spectral backscattering and extinction coefficients. Extensive works of Müller et al. (1999, 2000) and Veselovskii et al. (2002, 2005) at the Leibniz Institute for Tropospheric Research (TROPOS) thoroughly investigated the advantage of multi-wavelength LIDAR measurements to provide a robust estimation of PSD and refractive index of particulate media. Jagodnicka et al. (2009) retrieved broad bimodal PSD from multi-wavelength LIDAR measurements from UV to near-infrared (NIR). With these different studies, the concept of spectral LIDAR has emerged as a robust tool to probe microphysical properties of particulate media (e.g. PSD) with less assumption or need of a priori knowledge. All these spectral LIDAR techniques use the advantages of multi-spectral information to enhance the retrieval of microphysical properties of particulate media in the atmosphere. Long range measurements can be achieved thanks to high power laser sources. This approach has a major drawback in that it uses fixed wavelengths and cannot be easily tuned to cover a broad field of applications.

The second option for spectral LIDAR is to use a single tunable laser source emitting light over a large spectral domain. Different solutions are under consideration. A first solution uses tunable laser. Early work of Mudd et al. (1982) investigated the spectral backscattering coefficients of aerosols in a chamber as a function of wavelength in the IR with a tunable carbon dioxide laser. Recent solutions based on tunable Optical Parametric Oscillator (OPO) lasers have been proposed to probe particulate media. For instance, a spectral short and middle wave infrared (SWIR/MWIR) LIDAR has been developed for standoff bio-agent cloud detection using simultaneous broadband DIfferential SCattering (DISC) (Lambert-Girard et al. 2012). A 1064 nm laser coupled with a tunable OPO is employed to generate a broadband light between 1.5 and 3.9 µm emitted towards a particulate media and a telescope measures the backscattered light at short range. Although these novel techniques cover a relatively narrow bandwidth, they have the advantage of ranging profiles at long distances and being versatile for numerous applications.

The third option for spectral LIDAR is to use broadband light sources with lower power such as SC laser sources, which generate directional broadband light using cascaded nonlinear optical interactions in an optical fiber framework (Alfano and Shapiro 1970a, b). In spite of their limited peak power and beam quality compared with OPO laser sources, the feasibility of using SC laser sources for spectral LIDAR has been proposed. Spectral LIDAR signals have been measured in the NIR-SWIR domain up to 4 km in altitude using high peak-power by femtosecond-terawatt-laser sources (Méjean et al. 2003). Spectral LIDAR has been considered for identification of solid targets both indoors and in the field with a range up to 1.5 km from moderate peak-power SC sources (Manninen et al. 2014). The main limitation of this approach remains in the lack of available high power SC laser sources, which limits the maximum range.

In biomedical research, the propagation of light through biomaterials such as tissues is a complex problem. Light can be scattered by cell organelles (e.g. nuclei, mitochondria) with relative complex refractive indices different from the host medium (e.g. cytoplasm). The cell nuclei are appreciably larger than the optical wavelength (typically 5–10 m vs. 0.5 m) and scatter light in the forward direction, and there is significant scattering in the backward direction (Brunsting and Mullaney 1974; Mourant et al. 1998). Light-scattering by tissues have been extensively studied both experimentally and theoretically. Early work of Perelman et al. (1998) reported multi-spectral unpolarized measurements in order to retrieve the size distribution and density of epithelial nuclei. The wavelength dependence of the intensity of the light elastically scattered by the tissue structure was found to be sensitive to changes in tissue morphology, for instance for precancerous lesions. It was reported that specific features of malignant cells, such as increased nuclear size and nuclear/cytoplasmic ratio, could be retrieved from spectral light-scattering.

Spectral light-scattering, also named Light-Scattering Spectroscopy (LSS), by tissues have been proposed to extract and quantify morphological changes taking place during a disease, even at early stages of cancer for instance. The advantage of spectral light-scattering was shown on dysplastic human tissues using in the visible spectrum (Ghosh et al. 2011). The spectral correlation matrices presented in Fig. 2.5 were computed to probe scatterers of different sizes from small intracellular organelles, which strongly influence in the backscattering, to large nuclei, which influence in the forward scattering. From such analysis, normal and dysplastic tissues could be distinguished. LSS techniques have also been used to analyze and retrieve the properties of particles and particulate media from single microorganisms to complex cellular structures and tissues. The analysis of the spectral scattered light was carried out using different methods to extract self-similarities at varying scales associated with the structural changes (Soni et al. 2011).

For instance, spectral Diffuse Optical Tomography (DOT) is a derivative of spectral light-scattering techniques, which consists in recovering the scattering and

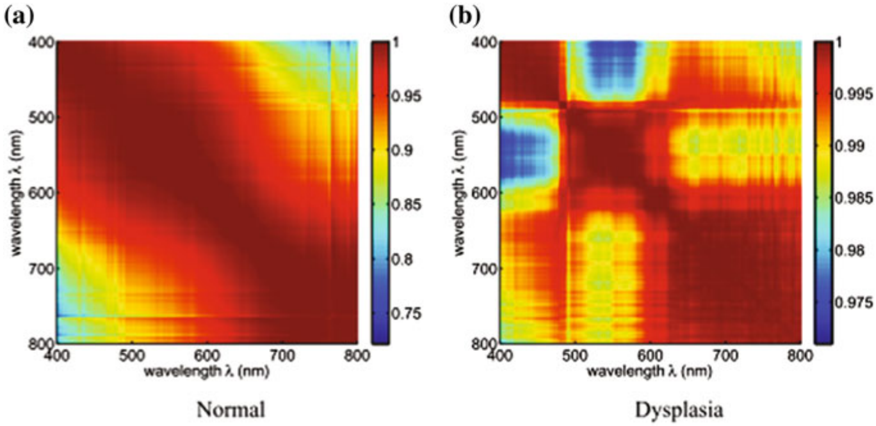

Fig. 2.5 Correlation matrices in the visible domain for (**a**) normal and (**b**) dysplastic samples (Ghosh et al. 2011)

absorption properties maps of tissues in function of time, space, and wavelength (Dehghani et al. 2003). With increasing number of wavelengths, modern systems have proved the ability to recover more physiologically relevant parameters; specifically, concentrations of species including oxygenated and deoxygenated hemoglobin, lipids, and water (Corlu et al. 2005, 2007). Because DOT requires the solution of an ill-posed scattering inverse problem, the utility of hyperspectral information (up to hundreds of wavelengths) has been demonstrated for diffuse optical tomography to recover concentration images of multiple chromophores (Larusson et al. 2011a, b). Another growing area of applications of spectral light-scattering involves the use of metal nanoparticles to form plasmonic hot spots for applications in biology or medicine (Patskovsky et al. 2014; Ray 2016).

In a nutshell, spectral light-scattering techniques have demonstrated their ability to improve optical characterization of particulate media. A significant amount of information provided by these techniques has been useful to solve numerous scattering problems in various fields of interest. However, most of them rely on numerous assumptions, such as the spherical or spheroidal approximations, to reproduce the light-scattering properties of dust particles for instance (Dubovik et al. 2006). For LIDAR observations, these strong assumptions, in addition to a poor understanding of light-scattering properties by irregularly shaped particles, may lead to a lower estimation of backscattering coefficients (Mishchenko et al. 1997). As a consequence, the LIDAR ratio (i.e. extinction-to-backscattering coefficient) may be considerably higher for irregularly shaped particles (e.g. mineral dust, aggregates) than for spherical particles. It may lead to significant errors for the retrieval of microphysical properties of irregularly shaped particles. The development of polarimetric light-scattering offers new ways to investigate particulate media composed of irregularly shaped particles.

In the following section, an overview of polarimetric light-scattering by particulate media is given. The advantages of studying light-scattering properties by accounting polarization states of light are discussed.

2.4 Polarimetric Light-Scattering

Polarization is a fundamental property of electromagnetic waves, which is modified by scattering depending on the microphysics of the particulate media. In that respect, knowledge of both intensity and polarization state of the scattered light may provide new possibilities for probing particulate media. Polarimetric effects are usually classified as: (i) diattenuation (i.e. differential attenuation of orthogonal polarization), (ii) retardance (i.e. de-phasing of orthogonal polarization), and (iii) depolarization (i.e. randomization of polarization state). Among these effects, much attention has been directed toward depolarization. For instance, multiple scattering induces a change of polarization state while the wave is scattered several times before detection. This modification of the polarization state may provide useful information about particulate media and could be used as an indicator of the particles concentration for instance. Different formalisms have been introduced to describe polarimetric light-scattering for optical and radar applications.

The *Jones formalism* was introduced (Jones 1941) to describe interactions between fully polarized electromagnetic waves and a medium. It is based on 2×1 Jones vectors $\mathbf{J} = (J_1, J_2)$ and 2×2 complex-valued dimensionless Jones scattering matrices $\mathbf{S}$ which operate both on the amplitude and the phase of the electromagnetic field as:

$$\mathbf{J_{sca}} = \mathbf{S} \cdot \mathbf{J_{inc}} = \begin{pmatrix} S_{11} & S_{12} \\ S_{21} & S_{22} \end{pmatrix} \cdot \mathbf{J_{inc}} \tag{2.1}$$

where $\mathbf{J_{inc}}$ and $\mathbf{J_{sca}}$ are respectively the incident and scattered Jones vectors and, S_{ij} are the complex elements of the Jones scattering matrix.

The *Stokes-Mueller formalism* was later introduced (Mueller 1943; Stokes 1852) to account partially polarized electromagnetic waves, which may arise from incoherent phenomena such as multiple scattering. Unlike Jones formalism, the Stokes-Mueller formalism relies on intensities rather than fields. It is based on 4×1 Stokes vectors $\mathbf{S} = (I, Q, U, V)^T$ (Stokes 1852) and 4×4 real-valued dimensionless Mueller matrices $\mathbf{M}$ (Mueller 1943) which both operate on intensities as:

$$\mathbf{S_{sca}} = \mathbf{M} \cdot \mathbf{S_{inc}} = \begin{pmatrix} M_{11} & M_{12} & M_{13} & M_{14} \\ M_{21} & M_{22} & M_{23} & M_{24} \\ M_{31} & M_{32} & M_{33} & M_{34} \\ M_{41} & M_{42} & M_{43} & M_{44} \end{pmatrix} \cdot \mathbf{S_{inc}} \tag{2.2}$$

where $\mathbf{S_{inc}}$ and $\mathbf{S_{sca}}$ are respectively the incident and scattered Stokes vector.

The Mueller matrix represents a complete polarimetric transfer function of a medium in its interactions with polarized light. An equivalent of the Mueller scattering matrix is defined as:

$$\mathbf{M} = \frac{\lambda^2}{4 \cdot \pi^2 \cdot D^2} \cdot \mathbf{F} = \frac{\lambda^2}{4 \cdot \pi^2 \cdot D^2} \cdot \begin{pmatrix} F_{11} & F_{12} & F_{13} & F_{14} \\ F_{21} & F_{22} & F_{23} & F_{24} \\ F_{31} & F_{32} & F_{33} & F_{34} \\ F_{41} & F_{42} & F_{43} & F_{44} \end{pmatrix} \tag{1.3}$$

where **F** is the 4×4 real-valued dimensionless phase matrix strongly dependent on the microphysical properties of the particles with diameter D. Generally, this matrix has non-zero values. The matrix can be significantly simplified for particles with a high degree of symmetry. Several elements of the matrix turn out to be equal to zero for randomly-oriented or axially symmetric particles (Van de Hulst 1981; Mishchenko et al. 2002). Different properties of the scattered Stokes vectors include the Degree Of Polarization (DOP), Degree Of Linear Polarization (DOLP), and Degree Of Circular Polarization (DOCP) as:

$$DOP = \frac{\sqrt{Q^2 + U^2 + V^2}}{I}; \quad DOLP = \frac{\sqrt{Q^2 + U^2}}{I}; \quad DOCP = \frac{V}{I} \tag{2.4}$$

Polarimetric light-scattering is generally categorized into two different methods. The first category, here stated as *polarimetric contrast-enhancing methods,* relies on the gating ability of polarization to subtract diffuse waves so as to enhance contrast. Thus, only single scattered light contribution can be extracted, yet maintaining a high DOP. Numerous techniques based on this method have been proposed to enhance the imaging quality of optical systems from simple techniques to advanced ones that maximize polarimetric contrast with adapted and predetermined polarization states to show distinctive polarimetric features (Richert et al. 2009; Upadhyay et al. 2011). The second category, here stated as *polarimetric quantitative methods*, actually exploits the comprehensive information from the complete Mueller matrix using different polarization sensitive sensors. The polarization-preserving but also the cross-polarized or co-polarized components can be used to infer microphysical properties of particulate media such particle size or shape (Mishchenko et al. 1995; Tishkovets et al. 2004). The latter category is of great interest for optical diagnostic of particulate media.

Inferring information from polarimetric light-scattering from particulate media is a complex and challenging task. First attempts have been undertaken by interpreting polarimetric data without properly modeling multiple scattering. Solutions provided by the Lorenz-Mie theory take into account polarization but are restricted to a single particle and effects such as depolarization induced by multiple scattering are not modeled. Most of these attempts led to large errors until multiple scattering was actually taken into account. Lyot in 1929 has called attention to the fact that the multiple-scattering DOP (i.e. resulting as the sum of all orders of scattering) is smaller than the single scattering DOP in a proportional manner. Van de Hulst

(1981) suggested that all the scattering of orders larger than the 1st order could be considered unpolarized. This simplistic approximation was proven to lead to significant errors. Hovenier (1971) later proposed a second approximation that all the scattering of orders larger than the 2nd order is unpolarized. This approximation results in taking into account only first and second order of scattering to model multiple-scattering. While this approximation results in better agreement with measurements, it still leads to significant errors. All the scattering orders must be taken into account to model polarimetric light-scattering accurately.

In astrophysics, early studies were conducted to understand the polarimetric signature of the scattered light from planetary regolith such as the Moon (Dollfus and Bowell 1971). Major polarimetry studies date back to the 1840s in France (Arago 1842; Lyot 1929) and later in USSR (Barabashev 1926). From astronomical observations, an inverse correlation was noticed empirically in 1912 between the surface albedo and the DOP of the light scattered by the lunar surface at large phase angles (Umov 1912). This so-called *albedo-polarization law* has been later corrected with further polarimetric measurements on many particulate surfaces and regolith (Dollfus 1971; Dollfus 1957; Bowell et al. 1972; Shkuratov 1980). A brightness enhancement toward exact backscattering direction and a branch of negative polarization (i.e. decreasing DOP reaching a minimum negative value at a small phase angle) were also measured for many particulate media. Continuing simulations progress has been made to explain these phenomena with mechanisms (e.g. coherent backscattering or shadow hiding opposition effect) to interpret photometric and polarimetric measurements of light-scattering by regolith and particulate media (Wolff 1975; Shkuratov 1981; Shkuratov et al. 1994; Zhang and Voss 2009).

Different techniques have been developed to compute polarimetric light-scattering with no limitation in terms of scattering orders, although the original Lorenz-Mie theory has been extended to systems of regularly shaped particles. For instance, the well-established RTT (Lommel 1889; Schuster 1905; Van de Hulst 1981; Chandrasekhar 1950; Ambartsumian 1957) has been extended from a scalar equation to a vector equation to include polarization (Evans and Stephen 1991). The Vector Radiative Transfer Equation (VRTE) fully models the transformation of the Stokes vector of electromagnetic waves due to its propagation and scattering in a medium. It is used to evaluate the solution of scattering problems in a polarimetric framework and gave good agreement with experiments for particulate media with multiple scattering (Riviere et al. 2013).

Techniques to measure polarimetric light-scattering have been developed since 1960s. These techniques investigate how a collimated beam of light is scattered at different angles by particulate media such as aerosols. Different categories of instruments have been considered. Polarization sensitive nephelometers or goniometers have permitted to measure the complete or partial Mueller matrix of single particles or particulate media (e.g. water, quartz, silica, dust) (Pritchard and Elliott 1960; Holland and Gagne 1970; Weiss-Wrana 1983; Kuik et al. 1991; Muñoz et al. 2000). Other instruments consider limited angular range such as forward-scattering (Eiden 1966; Gramm et al. 1974a, b). Angular information from light-scattering is mostly sensitive to the particles size and relative complex refractive index, while polarization is very sensitive to particles shape and relative complex refractive index (Ward et al. 1973; Tanaka et al. 1982; Zhao et al. 1997). When compared with Lorenz-Mie's solutions for homogenous spheres, good agreement was reported at forward scattering angles. However, significant errors are identified at backscattering angles, which may be reduced by increasing the particles absorption coefficients (Holland and Gagne 1970). This example illustrates how inferring particles relative complex refractive index can be difficult for single-wavelength polarimetric light-scattering, especially when only backscattered light is measured. The problem of estimating microphysical properties using angular and polarimetric light-scattering often remains an ill-posed problem in numerous scientific fields.

Polarimetric light-scattering has been neglected in the past decades for numerous applications in remote-sensing while it offers an interesting tool to probe the earth's atmosphere. The light becomes partially polarized as it is scattered by the molecules and aerosols in the atmosphere, whereas the direct sunlight is unpolarized. The polarization of skylight follows the well-established theory of Rayleigh scattering in a molecular atmosphere, with anomalies measured in unclear atmosphere caused by aerosols. Long after the hypothetic use of a dichroic material by the Vikings for navigation (Roslund and Beckman 1994), qualitative measurements of the skylight were first achieved at the beginning of the nineteenth century by Arago (1858). For several decades, most polarimetric measurements used unpolarized natural light sources and remained passive remote-sensing techniques. Pioneer quantitative polarimetric light-scattering measurements of the atmosphere, i.e. DOP of skylight, were carried out before the 1960s by visual polarimeters (Comu 1890; Pyaskovskaya-Fesenkova 1958) and later with increased accuracy using electronic devices in clear and polluted atmospheric conditions (Tousey and Hulburt 1947; Sekera 1957; Hariharan and Sekera 1966; Sun et al. 2014a, b), including polarimetric twilight sky measurements (Fesenkov 1966; Rozenberg 1968). For cloud research, an important challenge is to discriminate liquid water from ice water clouds. Polarimetric information has become a valuable mean to remotely sense the shape of aerosols. In that respect, numerous studies have proved that liquid water droplets and ice water particles exhibit different polarimetric light-scattering signatures, which depends on cloud microphysics and optical properties. The use of passive polarimetric remote sensing began in the 1970s including polarimetric light-scattering measurements from high-altitude balloon flights to distinguish liquid water clouds from ice water ones (Bums 1975; Stowe 1977).

A Swedish-built UV spectropolarimeter was launched on a Soviet satellite in the Intercosmos series to record resonance-line polarization in the solar spectrum around 130–150 nm (Stenflo et al. 1976). Further polarimetric measurements were carried out around 1980s in the Pioneer Venus Orbiter (Travis 1979) and the Space Shuttle (NASA) (Whitehead 1990). Later, the POLarization and Directionality of the Earth's Reflectance (POLDER) instrument (CNES, France) was a spaceborne polarimetric sensor launched in 1996 to collect polarized and directional solar radiation from space (Deschamps et al. 2002). Simultaneous retrieval of the particle size and shape was achieved from POLDER simulations and measurements (Goloub et al. 1994; Breon and Goloub 1998). For instance, polarimetric features such as zero polarization (between 75° and 120° from the incoming direction) and polarization maximum (around 140°) were used respectively to infer the effective radius of cloud droplets and type of clouds (either liquid or ice water phase) by Sun et al. (2015a, b).

Active polarimetric remote-sensing have emerged from the mid-1960s with early work of Rozenberg who has investigated polarimetric light-scattering at night-time using an artificial illumination of the atmosphere and polarization sensitive sensors (Rozenberg 1968). Although the invention of laser opened new possibilities to sense particulate media in the atmosphere, active remote-sensing techniques such as LIDAR did not exploit polarization at first. Polarimetric LIDAR was proposed to profile and characterize aerosols in the atmosphere as polarimetric measurements provide information about the shape of particles (Schotland et al. 1971; McNeil and Carswell 1975; Sassen 1991; Murayama 1996). Polarimetric LIDAR has shown its ability to distinguish spherical particles from irregularly shaped particles from depolarization measurements (Sassen 1991; Mishchenko and Sassen 1998; Sassen et al. 2007). This category of LIDAR is also used to study clouds and, for instance, to distinguish ice clouds from water clouds (Ansmann et al. 2005) or stratospheric clouds (Reichardt et al. 2000). It has also been used to identify and discriminate different types of aerosols such as volcanic ash (Hayashida 1984; Sassen et al. 2007), dust (Gobbi et al. 2000), black carbon (Li et al. 2015), contrails (Freudenthaler et al. 1996), or aerosolized biological warfare agents (Richardson et al. 2008) from other aerosols present in the atmosphere.

In the field of biomedical studies, optical techniques mostly rely on photometric measurements without taking into account polarization effects (Boas et al. 2011). Early works from 1980s have shown that polarization could be a sensitive tool to investigate the modification of tissues, bacterial suspensions, or blood cells (Johnston et al. 1988; Van de Merwe et al. 1989; Gross et al. 1991). Polarimetric light-scattering techniques range from the simplest to the most comprehensive, including ellipsometry (Dreher et al. 1992), fluorescence (Mohanty et al. 2001), Mueller matrix imaging (Dreher et al. 1992), or full Mueller endoscopy (Dreher et al. 1992). Although most techniques usually use polarization gating capabilities as a way to reduce multiple-scattering effects and improve signal-to-noise ratio, a category of techniques fully exploits polarimetric light-scattering. These methods are more comprehensive and complex by nature as it results in thorough interpretations of polarimetric measurements in order to extract useful information. It has been demonstrated that polarization could sense structural changes in malignant tissues as compared to the healthy tissues for diagnosing diseases (Bordier et al. 2008; Ghosh et al. 2009) or cancerous cells (Anastasiadou et al. 2008) for biomedical diagnosis. Despite polarimetric light-scattering gains interest in biomedical fields, several strong challenges and limitations remain. Simultaneous occurrences of polarization effects (e.g. diattenuation or retardance) is a serious challenge for polarimetric light-scattering as it may alter the measured signal, which can lead to erroneous estimation of the polarization-preserving signal (Ghosh 2010).

In a nutshell, polarimetric light-scattering techniques provide useful additional information regarding particulate media, such as the shape, concentration, local organization, or orientation of particles. Merging directional and polarimetric light-scattering information has been useful to probe complex or dense particulate media such as clouds or tissues. However, most polarimetric light-scattering techniques often assume no spectral dispersion of the materials or change in particle size distribution. Such assumptions may lead to erroneous results from inverse methods. The development of spectral and polarimetric light-scattering intend to offer a more robust and comprehensive method, without prior knowledge such as PSD or relative complex refractive index, to investigate complex particulate media, including particles with wide size distribution, materials with spectral dispersion, irregularly shaped particles, and dense media.

2.5 Spectral Polarimetric Light-Scattering

While several spectral or polarimetric methods have been proposed to study complex systems of small particles, the retrieval of the intrinsic microphysical parameters of particulate media remains challenging without prior knowledge of the PSD or relative complex refractive index. Spectral and polarimetric light-scattering are both sensitive to different microphysical properties of particulate media. As a result, methods have been proposed to merge spectral and polarimetric properties of light-scattering (Thompson et al. 1980; Chen et al. 1988). The goal of these methods is to identify microphysical parameters of small particles and particulate media, without assumptions or a priori information. Besides, the merge of spectral and polarimetric light-scattering may yield complementary information to retrieve microphysical parameters of particulate media (Huckaby et al. 1994). This merge is expected to ease the retrieval of additional microphysical parameters of the particulate media, such as porosity, structuration, or compactness. All these terms refer to the way the particles are arranged within complex particles, aggregates or clusters for instance. This section presents a review of different emerging methods based on the fusion of spectral and polarimetric light-scattering, also referred as polarized spectroscopy, spectral Mueller matrix analysis, or spectro-polarimetry.

By merging spectral and polarimetric information from light-scattering, one can compute the spectral DOP for particulate media. The spectral DOP is retrieved from perpendicular and parallel polarized intensities as:

$$DOP(\lambda, \theta) = \frac{I_P(\lambda, \theta) - I_S(\lambda, \theta)}{I_P(\lambda, \theta) + I_S(\lambda, \theta)} \tag{2.5}$$

where λ refers to the wavelength and θ to the scattering angle.

The spectral DOP is also a wavelength-dependent polarimetric contrast between two p and s orthogonal states of polarization. The variation of the spectral DOP originates from complex electromagnetic phenomena between particles:

i. *Light-absorption by the particles*. Absorption is the predominant phenomenon to explain the wavelength-dependence of the spectral DOP. For instance, when polarized light is scattered at absorbing wavelengths, the light is strongly absorbed and the spectral DOP is significantly enhanced at these wavelengths.
ii. *Multiple-scattering by particles*. This is another important phenomenon that explains the wavelength-dependence of polarization. The general idea lies in the fact that light-scattering by particles is conditioned by the range of electromagnetic interactions. This interaction range is directly related to the x-parameter, i.e. the ratio between the particle size and wavelength. For a given particle size, the range is minimal for x-parameter close to unity, whereas the range increases for larger values of x. Depending on the number of neighbor's particles involved in the interaction range, multiple scattering events may occur. Spectro-polarimetric light-scattering results from the number of particles covered by one wavelength, which causes multiple scattering and depolarization. Hence for a broadband light source, the part of multiple scattering, and as a consequence depolarization, varies with the wavelength.
iii. *Spectral dependence of polarimetric effects*. Effects such as diattenuation or retardance may be used in combination with the wavelength-dependence of depolarization for comprehensive assessment of particulate media.

Consequently, the variation of the spectral DOP results in a *spectral gradient of degree of polarization* $\nabla DOP(\lambda, \theta)$. This gradient is directly computed from the spectral DOP when spectral data are available, for instance from multi-spectral or hyperspectral sensors. In a similar way with the spectral slope or spectral gradient for reflectance, this spectral gradient of DOP is defined as:

$$\nabla DOP(\lambda, \theta) = \frac{dP(\lambda, \theta)}{d\lambda} \tag{2.6}$$

The spectral gradient of DOP, qualified as positive or negative regarding the sign of the gradient with the wavelength, turns out to be a promising tool for sensing distinctive features related to the microphysics of particulate media and studying the inner structure of complex clusters of particles. In regard to the implication of the merging spectral and polarimetric information from light-scattering, a broad spectrum of applications has emerged from aerosols characterization (Farhoud 1999) to purity of nanoparticles by Barreda et al. (2015a, b).

Remote-sensing has recently and progressively merged spectral and polarimetric light-scattering techniques to probe particulate media remotely. Farhoud (1999) has measured from spectro-polarimetric light-scattering a wavelength-dependence of the spectral DOLP and revealed a minimum polarization for aerosols characterization. In passive remote-sensing, the spectral polarization of clear and hazy daytime sky was retrieved from simultaneous spectral irradiances measurements at high spectral and angular resolutions. Such analysis combined with spectro-polarimetric RTT has revealed the combined angular and spectral effects of light-scattering on DOP. It could provide useful quantitative insights into how polarimetric spectra depend on scattering and absorption by tropospheric haze droplets and other aerosols (Suzuki et al. 1997; Lee and Samudio 2012; Ejeta et al. 2012; Hollstein et al. 2009; Boesche et al. 2006). For instance, Sun et al. (2013a, b, c) investigated the role of air bubbles and brine pockets contained in sea-ice and lake-ice from spectral polarized reflectance and DOLP. In active remote-sensing, most techniques require additional information regarding the aerosols to inverse the well-known LIDAR equations, due to ill-posed LIDAR problem. Such additional information may come from prior knowledge of the aerosols or from measurements provided by passive (e.g. sunphotometer) instruments, in which particles are collected and analyzed to determine their size, composition or morphology. The idea of merging spectral and polarimetric light-scattering information appears promising for future LIDAR applications.

Few studies have used multi-wavelength and polarization data for estimating the aerosol properties (Groß et al. 2011). It has been showed that using measurements at two wavelengths helps to distinguish different types of aerosol (Sugimoto and Lee 2006), most LIDAR systems employ only one wavelength for the analysis of the particle linear depolarization ratio of dust by Sassen (1991, 2007). From simulations, Sakai et al. (2007) studied the relationship between the wavelength-dependence of the backscattering coefficients and the depolarization ratio measured by LIDAR at multiple wavelengths. Several light-scattering calculations have shown that the spectral dependence of depolarization depends on the size distribution of non-spherical particles and could be used by Mishchenko and Sassen (1998) and Wiegner et al. (2009). The development of multi-wavelength polarization Raman LIDAR in the mid-1990s was one important step in our ability to characterize mineral dust particles (Müller et al. 1998; Althausen et al. 2000; Veselovskii et al. 2002). First, dual-wavelength aerosol polarimetric LIDAR measurements were carried out by Sugimoto et al. (2002), followed by multi-wavelength measurements of the linear depolarization ratio by Freudenthaler et al. (2009). The Cloud-Aerosol Lidar and Infrared Pathfinder Satellite Observations (CALIPSO, NASA-CNES) (Winker et al. 2003) is a satellite mission with a unique payload consisting in a two-wavelength polarimetric spaceborne LIDAR (CALIOP). These measurements provide information on the vertical distributions of aerosols and clouds, identification of water/ice cloud (from the depolarization ratio provided by the two orthogonal polarization channels), and a classification of aerosol PSD (from the wavelength-dependence of the backscattering coefficient). These multispectral polarimetric LIDAR measurements were exploited to improve inverse schemes and to retrieve microphysical properties of aerosols (Dubovik et al. 2006; Müller et al. 2013). Most of these spectro-polarimetric light-scattering based remote-sensing techniques are non-imaging techniques (Goldstein and Chenault 2002). Several imaging techniques have been proposed to exploit the advantages of merging polarimetric and spectral reflectance to enhance the contrast of man-made surface in a scene embedded or not in turbid media (Johnson et al. 1999; Le Hors et al. 2000; Giakos 2006; Wang et al. 2007).

In astrophysics or cosmology, spectral DOP, also called *polarimetric colors*, were measured at different wavelengths and polarization states for a variety of particles in space and particulate media such as planetary regolith surfaces. In the mid-1950s, first multispectral polarimetric measurements of the Moon noticed a wavelength dependence of the polarization (Dollfus 1957). Further measurements later corroborated these results on lunar regolith and solid lava fragments (Coffeen 1964). Lunar regolith appears to exhibit both wavelength and phase dependency of the polarization, while no wavelength dependence was reported for solid lava fragments. These studies are considered among the first publications suggesting the potential of merging spectral and polarimetric light-scattering to identify micro-physical properties of particulate media. Spectro-polarimetric light-scattering properties of cosmic dust are hard to measure and, in most studies, only multi-spectral data are available (Myers and Nordsieck 1984; Le Borgne et al. 1987; Chernova et al. 1993; Crovisier et al. 1997; Kiselev et al. 2000). When measurements at different wavelengths are available, the spectral gradient was found to differ significantly for different particles such as comets, dust, or asteroids. Regarding spectral DOP, positive or negative colors refer to the sign of the spectral gradient: for instance, positive color refers to positive spectral gradient values. Asteroid regolith often exhibits negative color, which may result from their high compactness while most comic dust exhibits positive polarimetric color due to their high porosity. Kolokova modeled accurately electromagnetic interactions between the small particles of cosmic dust aggregates with different particles arrangement or porosity (Kolokolova and Jockers 1997; Gustafson and Kolokolova 1999; Kimura 2003; Kolokolova 2010, 2016). Their results have shown a high dependence of the spectro-polarimetric light-scattering properties on their porosity. This relationship originates from electromagnetic interactions, which contribute directly to the polarimetric color. Ceolato et al. (2013) simulated broadband spectral and polarimetric light-scattering by small particles aggregates and super-aggregates. It has been reported significant dependence of the aggregate parameters upon the spectro-polarimetric light-scattering signatures. Other laboratory measurements have confirmed singular differences in the spectral DOP for natural particulate surfaces such as planetary regolith or artificial powders (Sun et al. 2014a, b). As reported by these different studies, the number of particles per single wavelength, as well as the ratio between the gyration radius and the wavelength, is significant parameters which influence the spectro-polarimetric light-scattering by aggregates. This ratio mainly governs the influence of the structure of the aggregate upon spectro-polarimetric light-scattering: for small values, the influence of the structure is negligible, whereas, for large values, the structure becomes a governing factor of the signature. Spectral dependence of the DOLP was measured as well as an increase within absorption bands, where the reflectance decreases sharply.

Early studies in astrobiology have proposed that the wavelength-dependence of polarization of light could be a key to detecting life traces in the universe and distinguishing them from non-biological species (Pospergelis 1969; Wolstencroft 1974). These broadband polarimetric features, resulting from the homochiral nature of the organics, are proposed as signatures of life called *bio-signatures* (Sparks et al. 2009;

Sterzik and Palle 2012; Berdyugina et al. 2016). Circular polarization of light, in particular, was found to be not only non-zero but to vary distinctly with the wavelength within high absorption bands, depending on the number and size of particles forming an aggregate of chloroplasts (Nagdimunov 2013). These studies showed that the more compact the aggregates, the more polarized is the scattered light, in a similar way to what has been studied for comic dust.

Biomedical research has been intensively active in merging spectral and polarimetric properties of light-scattering. Apart from techniques where polarization is used to suppress multiple-scattering from spectral light-scattering (Sokolov 1999), polarimetric spectra of biological tissues were found to be strongly influenced by cell nuclei morphology and constituents. Skin and tissues are subject to morphological, functional state, and structure modifications by different pathologies. These spectro-polarimetric modifications may imply changes of birefringence and structure, which can be accurately monitored by the spectral and polarimetric light-scattering (Sokolov 1999; Gurjar et al. 2001; Mourant et al. 2002; Zimnyakov et al. 2005). Pioneer work of Backman in 1999 proposed to measure both spectral and polarimetric light-scattering for quantitative analysis of biological samples. The proposed technique uses a broadband tungsten lamp and polarizers with multichannel spectrometers to measure the wavelength dependence of the polarized backscattered light in order to determine the size and relative complex refractive index of cell nuclei (Backman et al. 1999). Merging spectral and polarization information provided a robust method of removing the diffuse component of the scattered light. The residual spectrum is mainly composed of light from single backscattering and provides histological information about the epithelial cells and can be used to extract the size distribution, population density, and relative complex refractive index of the nuclei by comparison with Lorenz-Mie theory. This method was proposed to detect and diagnose precancerous changes in tissues and demonstrated the potential of spectro-polarimetric light-scattering to provide accurate quantitative estimates of the size distributions of cell nuclei and additional information, such as relative complex refractive index of cell organelles, which are very difficult to obtain using existing methods. In the recent years, the use of spectro-polarimetric light scattering to probe the morphological and structural changes of cells has become an active field of research. Different theoretical models were proposed based on Lorenz-Mie theory to analyze the single backscattering polarimetric spectra. For instance, a two-layered model was used to retrieve morphological parameters related to the abnormality of biological tissues, including the mean diameter, size distribution and relative complex refractive index (Zhao et al. 2014). Several techniques from laboratory have investigated the dependence of the spectro-polarimetric light-scattering on these parameters to endoscopic measurements (Ding et al. 2007; Qi et al. 2012). Results indicate that the angle of maximum depolarization shifts toward larger values as the wavelength decreases from IR to UV (Ding 2007). Even though the angular shift is relatively small, it is sufficient to exhibit a high correlation with wavelength. Similar results were later reported using a broadband laser source for cancerous cells (Ceolato et al. 2013). A major advantage of merging spectral and polarimetric information is to be able to probe complex biological systems. Spectro-polarimetric measurements were carried out on bacteria colonies under different environments, and inverse power-law dependence over a broad range of wavelengths was extracted from the fractal analysis (Banerjee et al. 2013).

From a medical diagnostic perspective, the potential use of spectral polarimetry was proposed to detect different pathologies such as leukemia, in which red blood cells decrease in numbers as a result of an abnormal proliferation of white blood cells. Red blood cells are known to play a major role in the absorption and scattering properties of blood (Tuchin 1997). Their variation in numbers in the blood may infer changes in the spectral polarimetric light-scattering signatures of blood. Recent results showed a strong depolarization of light by blood at 400–500 nm, where high absorption of hemoglobin may cause significant randomization of polarization (Swami et al. 2010). Spectro-polarimetric measurements have reported a minimum of depolarization of light which may be related to the number of red blood cells (Aziz et al. 2013). This minimum of depolarization has been proposed to be used for diagnosing acute lymphoblastic leukemia. Experimental results have suggested the potentials of the techniques based on the fusion of spectral and polarimetric light-scattering for skin pathological diagnosis and treatment evaluation. Ramella (2011) measured the full Stokes vectors of chicken muscle at several wavelengths in the visible domain. The change of depolarization with wavelength is also explained by a decrease of the blood hemoglobin absorption, which is the primary source of the light absorption in the visible wavelength range. Thus, the increase of light penetration depth enhances the scattering and leads to a larger depolarization of backscattered light for both healthy and cancerous tissues in the red part of the spectrum. Spectral Mueller matrix images of ex vivo human colon tissues revealed a contrast enhancement between healthy and cancerous zones of colon specimen compared to unpolarized intensity images (Novikova et al. 2014). Similar results were reported on mice melanoma using spectral polarimetric light-scattering measurements (Ceolato et al. 2015).

These early and recent works have demonstrated the advantage of coupling spectral and polarimetric methods for optical diagnostic of complex particulate media. In order to retrieve microphysical properties of these media, a comprehensive quantitative approach is required. In the next section, a complete experimental and numerical method is detailed to compute accurate spectro-polarimetric light-scattering signatures for a given particulate media.

2.6 Quantitative Spectro-Polarimetric Light-Scattering

ONERA, The French Aerospace Lab, has developed different experimental facilities for optical diagnostic of particulate media. A variety of systems, such as laser-based nephelometers or LIDAR, have been used for years for optical diagnostic of complex dense systems of particles (Hespel and Delfour 2000; D'Abzac et al. 2012; Ceolato et al. 2012). Based on recent developments in light-sources and optical-sensors, original concepts of optical characterization, including full spectral range, polarimetric, and high angular resolution, have been investigated to perform more robust, accurate, and comprehensive remote optical diagnostic. This section reports recent works dedicated to performing a quantitative analysis of spectro-polarimetric light-scattering. A systematic study aimed at searching the microphysical parameters characterizing particulate media has been engaged and are reviewed in this section.

Developments in nanostructured fiber optics and compact pulsed lasers have resulted in the conception of supercontinuum (SC) laser sources (Alfano and Shapiro 1970a, b). These sources are generated using a pulsed laser propagating through a non-linear medium. It results in a spectral broadening (Dudley et al. 2006) and the creation of "white" directional coherent light. SC lasers are directional and coherent light sources based on the supercontinuum generation phenomenon. Discovered in the 1970s, this phenomenon is the result of the propagation of intense narrow-band ultrashort laser pulses inside a material (e.g. optical fiber or bulk). This phenomenon broadens the spectrum of the single-frequency pulses (Alfano and Shapiro 1970a, b) and results in the generation of a broadband laser light. This spectral broadening is a typical nonlinear effect due to strong laser-field confinement and can extend from the IR to the visible. The intense pulse induces atomic or molecular modification of the material, which in turn varies the dispersion law by optical Kerr effects. The variation in relative refractive index produces non-linear phenomena resulting in the frequency sweep within the pulse by phase shift or self-phase modulation. Other more complex phenomena, such as stimulated Raman scattering and four-wave mixing (Coen et al. 2002) can also be involved. With the current progress in nanophotonics, new broadband laser sources are available based on SC generation from UV to IR. Ultrashort pulsed laser sources (e.g. femto or picosecond) are combined with Photonic Crystal Fibers (PCF), which are used as the propagating material. The PCF has a small core diameter and has a nonlinear coefficient that can be engineered to achieve a specific output spectrum (Ranka et al. 2000). The coherence properties of SC lasers have been investigated using spectral interferometry (Zeylikovich et al. 2005). Although they present a low temporal coherence, these sources yet retain a high degree of spatial coherence (Alfano and Shapiro 1970a, b).

In parallel, spectral or hyperspectral sensors have been used intensively for years in the remote-sensing community (Shaw et al. 1973a, b; Manolakis and Marden 2003). Sensing with a high spectral resolution consists in measuring the intensity of light over a wide range of wavelengths. This is accomplished by spectrophotometers or hyperspectral sensors, which have been used intensively in the remote-sensing community (Ientilucci 2009). Hyperspectral sensing refers to the measurement of light intensity for more than thousands of spectral bands. The outputs of hyperspectral sensors are tensors, or also named *hypercubes*, where the dimension is related to the number of bands. The combination of SC laser sources with hyperspectral sensors is of rising interest for a broad range of applications (Johnson et al. 1999; Peng and Lu 2008; Zakian et al. 2009; Larusson et al. 2011a, b; Hakala et al. 2012).

Rather than a single or multi-wavelength approach, a spectro-polarimetric laser-based scatterometer was designed at ONERA to characterize particulate media. One advantage of spectro-polarimetric light-scattering measurements performed by this scatterometer is to analyze the spectral dependence of various scattering media from rough surfaces to particulate media. The originality of the system is to use a SC laser source coupled with hyperspectral sensors. No monochromator is needed and the full polarimetric spectrum is measured at once. Hyperspectral, polarimetric, and directional light-scattering measurements are carried out simultaneously. This innovative instrument carries out in-line, and non-destructive remote optical measurements. This spectral polarimetric scatterometer measures the light scattering in visible and IR ranges (VIS/NIR/SWIR) from 480 to 2500 nm with a spectral resolution lower than 1 nm in the visible near-infrared range, and lower than 5 nm in the short-wave infrared (Riviere et al. 2012; Ceolato et al. 2012). A simplified schematic of the design of the MELOPEE scatterometer is presented in Fig. 2.6.

The incident lighting system consists of a SC laser combined with an achromatic collimator. The laser source is initially fully unpolarized at full power and is coupled to wide-band polarizers to select incident polarization states. The variation of the incident power is measured to quantify the stability of the laser source. The polarizers' efficiency was found to be greater than 98% on the whole spectral range. The sensing system consists of a CCD/InGaAs-sensor based spectrophotometer mounted on a goniometric platform at 1 m from the target. The instrument measures the scattered

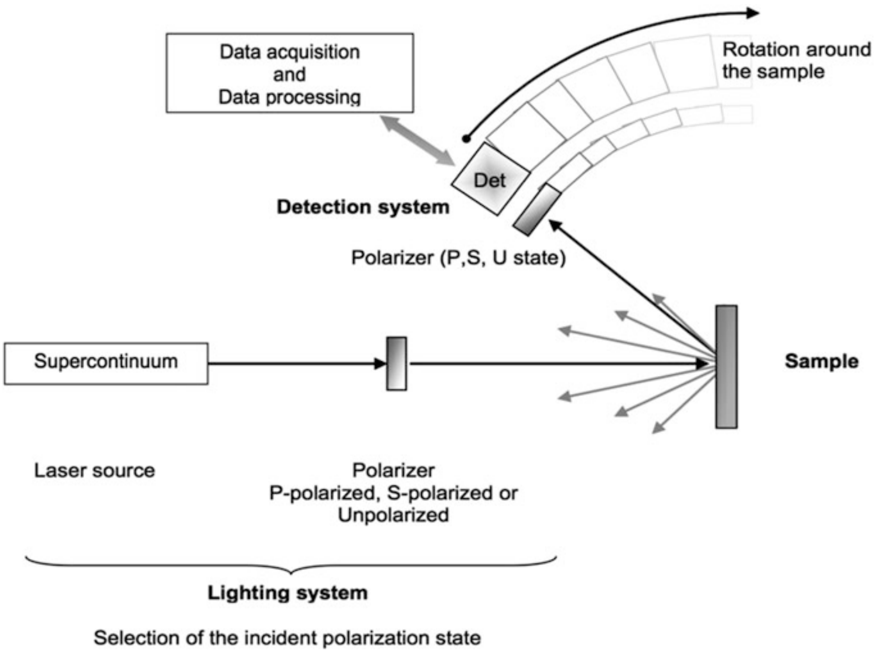

Fig. 2.6 Schematic of the VIS/NIR hyperspectral version of MELOPEE instrument developed at ONERA. The incident lighting system is a SC laser coupled to wide-band polarizers. The sensing system is composed of a CCD-based spectrophotometer mounted on a goniometric platform

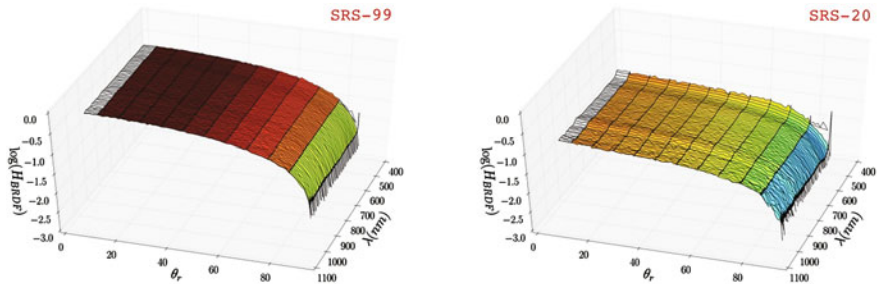

Fig. 2.7 Light-scattering measurements for Lambertian materials: Spectralon® SRS-99 and SRS-20. The illumination is P-polarized and the detection unpolarized

light with an azimuthal angular resolution of 0.1° and provides high angle-resolved measurements. A 5-axis fully automated sample holder facilitates the measurement procedure. For light-scattering measurements, the principal plane is defined as the plane that contains the normal of the sample and the incident beam. Both in and out of principal plane configurations are available with this scatterometer. Our instrument has been calibrated using different Lambertian reference standards such as LabSphere Spectralon®. Figure 2.7 presents the spectral and angular light-scattering measurements on LabSphere Spectralon® SRS-99 and SRS-20. These reference standards are found to behave closely as a Lambertian surface at normal angle of incidence from 480 to 1000 nm. Along with accurate spectro-polarimetric scatterometer, it is important to develop dedicated light-scattering models.

Along with MELOPEE scatterometer, ONERA has developped several numerical models to compute spectro-polarimetric light-scattering by a wide range of particulate media.

For particulate media composed of *axisymmetric particles* (e.g. spherical, spheroidal), a spectral and polarimetric RTT model was developed to model the spectro-polarimetric of dense particulate media. One essential condition for using the RTT approach to model multiple light-scattering by particulate media is that the distance d between particles must be larger than the wavelength λ such as $d > \lambda$. In such a way, the scattering events always occur in the far-field region of each particle and prevent coherent effects such as dependent scattering. This spectral and polarimetric RTT model solves the VRTE for an incident broadband illumination and spectral detection.

Let us first consider a particulate media as an ensemble of N particles in random orientations and positions in a non-scattering host medium. The spectral VRTE is given for a polarized broadband directional light source as:

$$\mathbf{u} \cdot \nabla \mathbf{S}(\mathbf{r}, \mathbf{u}, \lambda) + \mathbf{k_{ext}}(\mathbf{r}, \lambda) \cdot \mathbf{S}(\mathbf{r}, \mathbf{u}, \lambda) =$$
$$\frac{1}{4\pi} \cdot \int_0^{2\pi} \int_0^1 d\mathbf{u}' \cdot \mathbf{P}(\mathbf{r}, \mathbf{u}, \mathbf{u}', \lambda) \cdot \mathbf{k_{sca}}(\mathbf{r}, \mathbf{u}, \mathbf{u}', \lambda) \cdot \mathbf{S}(\mathbf{r}, \mathbf{u}', \lambda) + \mathbf{k_{abs}}(\mathbf{r}, \mathbf{u}, \lambda) \cdot \mathbf{S^0}(T) \tag{2.7}$$

where $\mathbf{k_{ext}}(\mathbf{r}, \lambda)$ and $\mathbf{k_{abs}}(\mathbf{r}, \mathbf{u}, \lambda)$ refers respectively the spectral extinction and absorption vectors. $\mathbf{k_{sca}}(\mathbf{r}, \mathbf{u}, \mathbf{u}', \lambda)$ refers to the spectral scattering matrix. $\mathbf{S^0}(T) = n^2 \cdot \sigma \cdot T^4/\pi$ is the total blackbody Stokes vector, T the temperature and $\sigma = 567051 \cdot 10^{-8} \mathrm{W} \cdot \mathrm{m}^{-2} \cdot \mathrm{K}^{-4}$ the Stefan-Boltzmann constant.

The spectral Stokes vectors $\mathbf{S}(\mathbf{r}, \mathbf{u}, \lambda)$ are the spectral VRTE solutions which encompass the spectro-polarimetric signatures of a particulate medium of interest as a function of position $\mathbf{r}$, direction $\mathbf{u}$, and wavelength λ. The phase matrix $\mathbf{P}(\mathbf{r}, \lambda)$ of an ensemble of particles is calculated by integrating the 4×4 real-valued dimensionless Mueller matrix elements $M_{ij}(r_p, \mathbf{r}, \lambda)$ over the PSD $n(r_p)$ of an ensemble (i and j range from 1 to 4):

$$\mathbf{P}(\mathbf{r}, \lambda) = \begin{pmatrix} P_{11} & P_{12} & P_{13} & P_{14} \\ P_{21} & P_{22} & P_{23} & P_{24} \\ P_{31} & P_{32} & P_{33} & P_{34} \\ P_{41} & P_{42} & P_{43} & P_{44} \end{pmatrix} \text{with}\, P_{ij}(r_p, \mathbf{r}, \lambda)$$
$$= \frac{\lambda}{\pi \cdot \mathbf{k}_{\mathbf{sca}}^2} \int dr_p \cdot M_{ij}(r_p, \mathbf{r}, \lambda) \cdot n(r_p) \tag{2.8}$$

Particulate media are modeled for numerical purposes as semi-infinite plane-parallel layers with constant radiative parameters as shown in Fig. 2.8. We consider multilayered isotropic scattering media. For instance, a particulate media

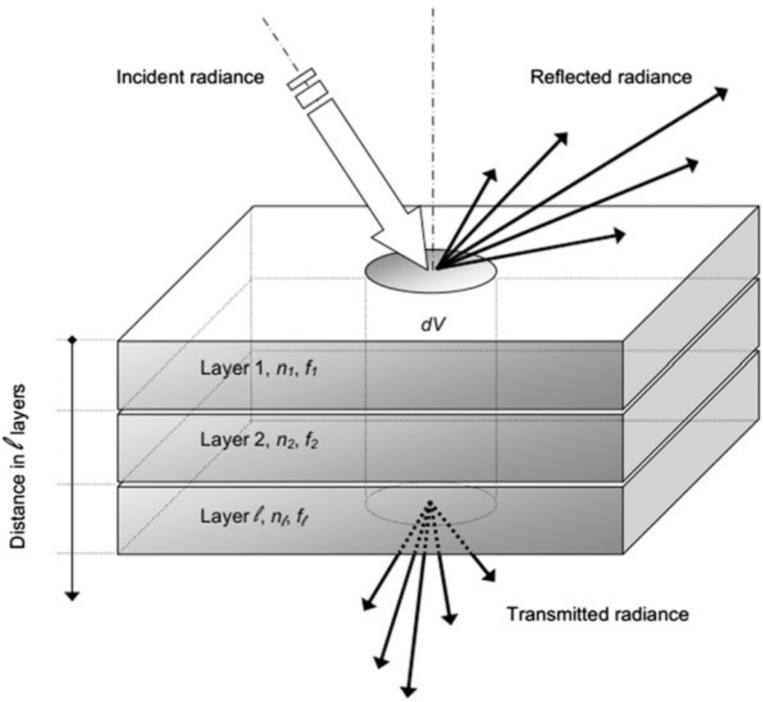

Fig. 2.8 Global view of the particulate media geometry and notation used for the simulation

inside a quartz or glass slab is modeled as a series of vertically inhomogeneous layers containing randomly oriented particles of various geometries. The general description of atmospheric layers is substituted herein by optical material interfaces, such as quartz or glass, with given relative complex refractive index. The extension of this model to spectro-polarimetric light-scattering requires several modifications including spectral dispersion of the interfaces or solving Fresnel equations at every interface for every wavelength.

Our model based on the spectral VRTE solves numerically a system of L equations, where L is the number of discrete wavelengths composing the broadband light source (typically $L = 2000$). The spectral operation consists of calculating the scattered spectral Stokes vector corresponding at each wavelength in the spectral range. Azimuthal angles are expressed as a Fourier series and polarization rotations are performed directly in azimuth space. Subsequently, Fourier transform is performed to retrieve the scattering matrix for each Fourier azimuth mode (Evans and Stephen 1991; Deuzé et al. 1989; Ishimaru et al. 1984). Multiple reflections between layers are also taken into account in the spectro-polarimetric radiance balance at the top and bottom of each layer. An adding-doubling technique is then deployed for each Fourier mode to model multiple scattering. This technique is numerically stable and is used to model multiple light-scattering in an intuitive, efficient, and simple way. A good selection of the Fourier modes and the quadratic angles for every wavelength is crucial for the computation.

Validation of the model has been carried out following a three-step procedure (Riviere et al. 2013). Briefly, (i) an analytical validation was conducted for Rayleigh scattering from Coulson's Table (1960), (ii) a stochastic method was used to validate the model for Mie scattering and, (iii) experiments were carried out on polystyrene particles in aqueous solution. As stated above, the spectral VRTE model is valid only for intermediate volume fractions, in dispersed-phase, as a large value of this parameter refers to a large number of multiple scattering events and multiple reflections inside a glass cuvette for instance.

Spectro-polarimetric light-scattering simulations are carried out using our spectral VRTE model for an incident broadband *p*-polarized collimated illumination. Typical radiative transfer inputs are optical thickness or albedo. However, for broadband calculations, these radiative parameters cannot be employed because of their spectral dependency. For broadband calculations, particulate media must be rather described in terms of microphysical parameters such as volume fraction or relative complex refractive index (both for particles and host medium), which are not dependent on the wavelength of illumination. Thus, a particulate media composed of an ensemble of random spherical particles is modeled with three principal microphysical parameters:

(1) *Particle size distribution*, which follows for instance a log-normal size distribution such as:

$$\frac{dn(rp)}{dr_p} = \frac{N_0}{r_p \cdot \ln(10) \cdot \sigma \cdot \sqrt{2\pi}} \cdot \exp\left(-\frac{\log(r_p/r_m)}{2 \cdot \sigma^2}\right) \tag{2.9}$$

where $n(r_p)$ is the PSD [$m^{-3} \cdot m^{-1}$], r_p the particle radius [m], N_o is the total number density of particles [m^{-3}], r_m is the mean particle radius [m], and σ is the standard deviation of distribution.

The *volume fraction* (Jeffrey and Acrivos 1976) describes the fraction of particles in the host media volume (e.g. air, liquid water). It is calculated from the *total particle volume* V_{part} [$m^3 \cdot m^{-3}$] for a given PSD by:

$$V_{part} = \int_{-\infty}^{\infty} \frac{\pi}{6} r_p^3 n(r_p) dr_p \tag{2.10}$$

(2) *Relative complex refractive index*, which accounts for the spectral dispersion and absorption of both particles and host media. Analytical refractive index models can be employed to compute spectral relative complex refractive index of materials.

In what follows, a particulate media composed of spherical silica particles is considered. The microphysical parameters for the simulation correspond to a mean radius r_m of 100 nm, a relative complex refractive index varying over the spectral range (e.g. $m = 1.59 + i\ 0.0$ at 532 nm), and a volume fraction of 1%.

The first and second elements of the spectral Stokes vectors are computed and presented in Fig. 2.9 against $\mu = \cos(\theta)$, the cosine of the scattering angle θ. The scattered intensity, related to the first Stokes matrix element I/I_{inc}, decreases for large wavelengths. This spectral dependence is shown in the backscattering ($\mu = -1$) and forward scattering ($\mu = +1$) directions. This dependence could be understood as the variation of the single-scattering efficiency over a broadband spectrum. The single-scattering efficiency is known to vary with the size parameter (i.e. ratio of the particle diameter to wavelength) (Mishchenko et al. 2002). Thus, it also varies when spectral scattered-intensities are computed over a wide spectral range for a fixed particle size (here, particle radius is fixed). The spectral DOLP, related to the second Stokes matrix element Q/I, also exhibits a clear spectral dependence especially for reflection angles (between $\mu = -1$ and $\mu = 0$). More interestingly, a noticeable feature is found around $\mu = -5$. It corresponds to a maximum depolarization where the spectral DOLP reaches low values. Similar features have been previously reported from experiments (Müller et al. 1998) and are further analyzed in the next section. A numerical artifact produces unrealistic values at $\mu = 0$.

The microphysical parameters of particles are expected to play a major role in the spectro-polarimetric light-scattering signatures of particulate media. A microphysical analysis is carried out to determine their impact on spectral polarimetric light-scattering signatures. Such analysis is a prior requirement in the development of specific inversion methods merging spectral and polarimetric

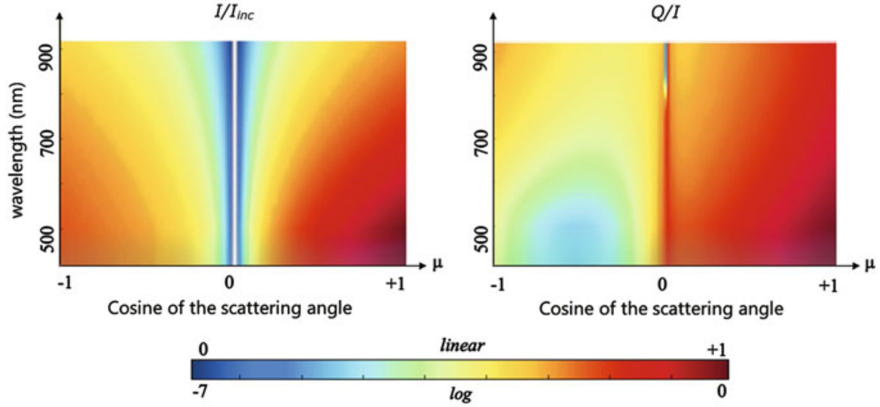

Fig. 2.9 Simulation of the spectral Stokes vectors (I/I_{inc} in log-scale and Q/I in linear-scale) scattered by a particulate medium for a broadband (480–1020 nm, with spectral resolution of 5 nm) p-polarized illumination

information. In the following, spectro-polarimetric light-scattering signatures are computed with different mean particle radius, relative complex refractive indexes, and volume fractions in the range of validity of the VRTE model. The mean particle radius ranges from 35 to 450 nm, the relative complex refractive index is constant over the spectral range with fixed values ranging from $1.5 + i0.0$ to $2.05 + i0.0$, and the volume fraction varies from 0.1 to 5.0%.

Figure 2.10 presents the spectral first Stokes elements (I/I_{inc}) resulting from multiple light-scattering by particulate media with varying microphysical parameters. They are plotted in log-scale for an incident broadband *p*-polarized collimated illumination and different sets of parameters. For each line, a single parameter varies when others remain constant. When not specified, the mean particle radius for a log-normal size distribution is $r_m = 100$ nm, the volume fraction is $f = 1.0\%$, and the relative complex refractive index is $m = 1.50 + i\ 0.0$.

Figure 2.11 presents the spectral second Stokes elements (Q/I) resulting from multiple light-scattering by particulate media with varying microphysical parameters. They are plotted for an incident broadband *p*-polarized collimated illumination and different sets of parameters. For each line, a single parameter varies when others remain constant, similarly to Fig. 2.10. In the figure, red color refers to polarized scattered light whereas blue color refers to unpolarized light: depolarization mainly appears in the backward scattering directions (from $\mu = -1$ to 0). For a given particulate media, depolarization is reported in the backward directions (from $\mu = -1$ to $\mu = 0$) and strongly depends on the wavelength. It shows a directional dependence and a spectral shift of the depolarization (i.e. low DOLP values).

Light-scattering by particulate media depend on the microphysical parameters of particles such as the particle size, relative complex refractive index, or volume fraction. Some of these parameters depends on the wavelength and may vary

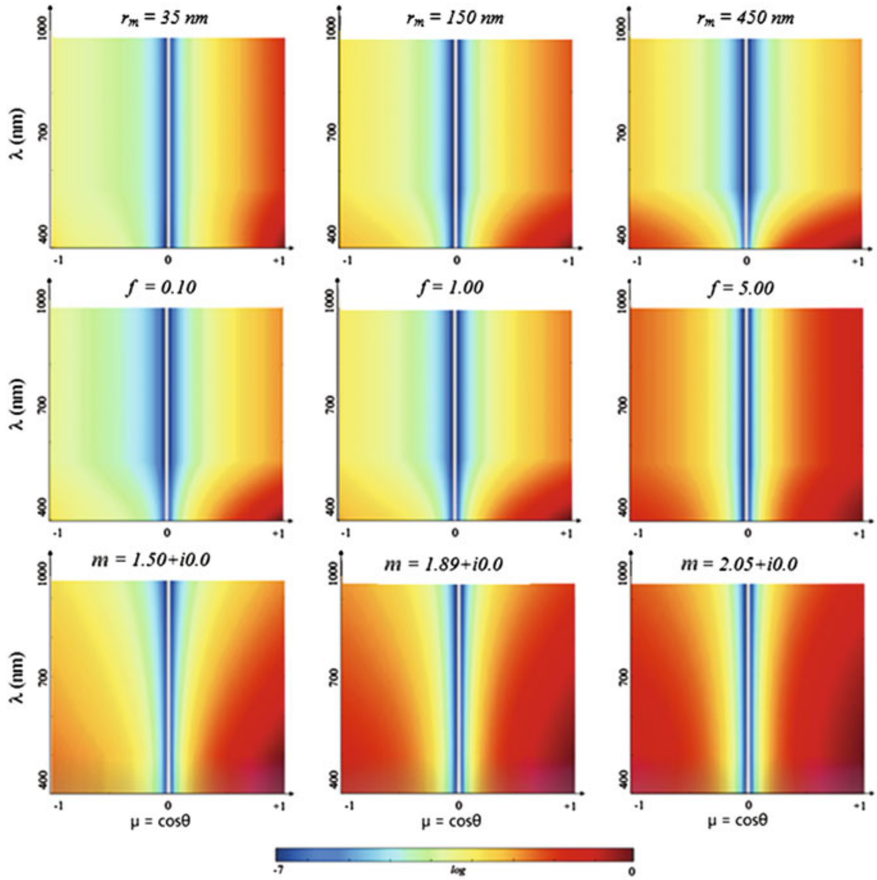

Fig. 2.10 Spectral computations of the first Stokes element (I/I_{inc}) in log-scale for an incident broadband (480–1020 nm, with spectral resolution of 5 nm) p-polarized collimated illumination. Variations of the mean particle size ($\underline{r_m}$), relative complex refractive index (m), and volume fraction (f) of particles

significantly for broadband calculation. Usual monochromatic light-scattering techniques investigate a single scattering regime. One advantage of spectral or broadband light-scattering computations is to address distinct scattering regimes for a given particulate media. From Fig. 2.10, a change of scattering regime is identified when the mean particle size or relative complex refractive index increases. However, no change is noticed for varying volume fraction. This is explained as the governing parameters of scattering (i.e. size and relative complex refractive index) are kept constant for different volume fractions. These results expose the interaction between microphysical parameters of particles and the wavelength of the light. Spectro-polarimetric light-scattering clearly provides interesting physical insights about the nature of particles in particulate media. Due to the interplay between the size and relative complex refractive index, using only the spectral scattering

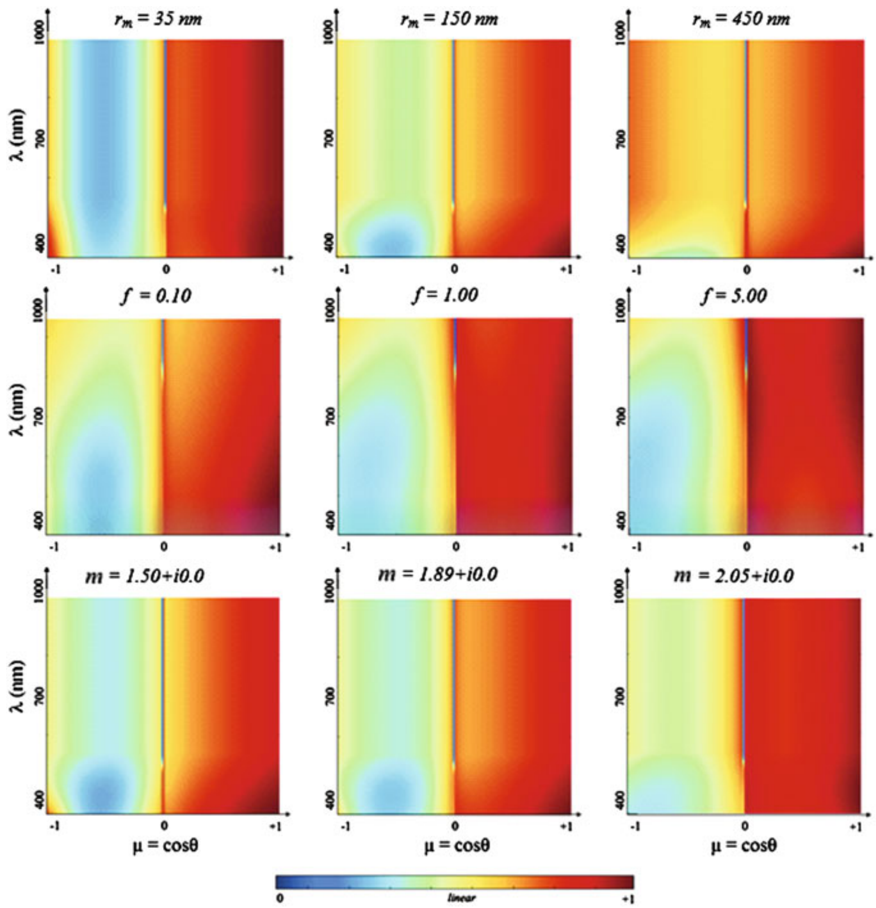

Fig. 2.11 Spectral computations of the second Stokes element (*Q*/*I*) for an incident broadband (480–1020 nm, with spectral resolution of 5 nm) p-polarized collimated illumination. Variations of the mean particle size (r_m), relative complex refractive index (m), and volume fraction (f) of particles

intensity may result in serious inversion hardships. The merge of spectral and polarimetric information is proposed by computing the spectral second Stokes vector element (*Q*/*I)* or the spectral DOLP. Depolarization from multiple scattering is a directional phenomenon (i.e. depends on the scattered angle) and can be simulated by our model over a wide spectral range from visible to near-infrared. As shown in Fig. 2.11, the incident polarization is conserved for transmission angles (including forward-scattering), whereas significant depolarization appears at reflection angles (including backward-scattering). Depolarization from multiple-scattering is known to depend on the particle size or relative complex refractive index (Kim and Moscoso 2001) and has been accurately computed by our model. When performing the microphysical analysis, the mean particle size, relative complex refractive index, and volume fraction are important factors that drive the spectral and directional depolarization at reflection angles.

For particulate media composed of *non-axisymmetric* particles (e.g. fractal aggregates), other numerical models must be considered. A Spectral Discrete Dipole Approximation (SDDA) model (Ceolato et al. 2013) was developed to compute the spectro-polarimetric light-scattering of fractal aggregates simulated by Diffusion-Limited Cluster-Aggregation (DLCA). The spectro-polarimetric scattered-light intensity curves were generated for coherent incident light with a wide spectrum ranging from the ultraviolet (UV) to the Short Wave Infrared (SWIR). In the DDA model, the aggregate is discretized on a cubic lattice, with each lattice being assigned an electric dipole that responds to the incident wave and couples to the other dipoles in the aggregate.

The accuracy of the SDDA model is then determined by the fineness of this discretization lattice (Yurkin and Hoekstra 2007). Applications often require computations for aggregates in random orientations. Consequently, we split our model into two operations: one is random orientation or orientational-averaging (Mishchenko and Yurkin 2017), and the other repeats the spectral calculations over the SWIR–UV wavelength range. The averaging operation consists of repeated calculations for the aggregate fixed in a set of equally probable random orientations following (Hage et al. 1991). This results in a statistical ensemble-average of a single aggregate morphology (Pathria 2003). However, rotating the aggregate position relative to the dipole lattice can produce so-called shape errors, which are orientation dependent (Mishchenko et al. 2006). It is preferable then to fix the DDA lattice to the aggregate and rotate the incident wave propagation and polarization directions while being careful to preserve the transverse nature of the wave. Other orientational-averaging schemes are possible such as analytical methods (Khlebstov 2001) and numerical evaluation using the T-Matrix that is retrieved from the DDA (Mackowski 2002). The spectral operation consists of calculating the scattered-intensities for wavelengths in the spectral range. To account for spectral dispersion, we use the Sellmeier dispersion equation (Sellmeier 1871) to model, in this case, the spectral properties of silica. This method could be widely extended to other aerosols such as soot particles.

The SDDA simulations are performed in the horizontal scattering plane, which is the plane perpendicular to the linear polarization of the incident wave. Spectro-polarimetric scattered intensity curves are calculated with 1° angular resolution and averaged over the 200–2000 nm spectrum with 5 nm spectral resolution.

Results from the SDDA model are presented for a standard aggregate and a superaggregate in both fixed and random orientations. The spectral and angular scattered-light intensities curves are plotted in Fig. 2.12 as a function of scattering angle and wavelength. Referring to Fig. 2.12a, c, which are for a fixed orientation, the scattered-intensities display differences in the forward and backward directions as the wavelength increases. In particular, there are distinct differences from 90° to 180° between the two aggregates. Figure 2.12b, d for averaged orientation shows similar features and can be directly compared to light scattering experimental measurements (Sorensen et al. 1992). The V-shaped appearance of the plots near

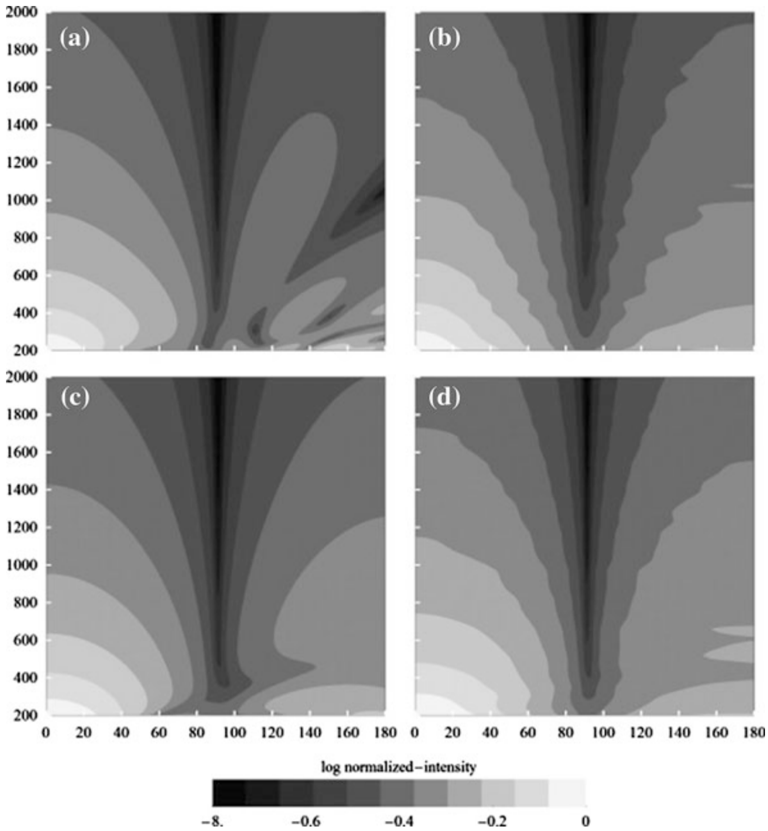

Fig. 2.12 Spectral angular-light-scattering for the silica aggregates. The scattered intensity is log normalized. Plots (**a**) and (**c**) show a fixed orientation for the standard and superaggregate, respectively. The corresponding orientational averaged plots are shown in (**b**) and (**d**)

90° is related to the first minimum after the Guinier crossover (Berg 2012). In addition, this feature persists after orientational averaging. Thus, this feature serves as a fingerprint, of sorts, independent of the aggregate's orientation. It may be that such fingerprints contain useful information about the aggregate morphology that would survive orientational averaging, and as such could find application in experimental characterization of aggregating particle-systems.

In a nutshell, spectro-polarimetric light-scattering by particulate media appears to present features related to distinctive microphysical parameters, such as:

1. *Mean particle size.* A spectral dependence of the depolarization on the mean particle size is reported. For constant relative complex refractive index and volume fraction, minimum DOLP values (i.e. maximum depolarization) appear around $\mu = -0.5$ and strongly varies with the wavelength and particles size. One can identify a limited spectral domain where the depolarization reaches a maximum value. This spectral domain is found variable from small particles to

large particles. Thus, this spectral feature would permit to identify the mean particle size of an unknown particulate media.

2. *Relative complex refractive index.* A directional dependence of the depolarization on the relative complex refractive index is reported. For constant particle size and volume fraction, a maximum depolarization appears around $\mu = -0.5$ and strongly varies with directions. The shape of the limited spectral domain with maximum depolarization is remarkably different when the relative complex refractive index varies. As relative complex refractive index increases, directions of maximum depolarization also increase. For instance, at $\mu = -1$ (in the perfect backscattering), DOLP ranges from 0.5 (i.e. partial depolarization) for $m = 1.59 + i\ 0.0$ to 0.1 (i.e. near complete depolarization) for $m = 2.05 + i\ 0.0$. This directional feature is proposed as a tool to probe the relative complex refractive index of particles composing an unknown particulate media.
3. *Volume fraction.* The limited spectral domain with maximum depolarization shows neither spectral nor directional dependence on volume fraction. However, a dependence of the minimum DOLP value on the volume fraction is reported. For a given particle size and relative complex refractive index, the minimum DOLP value varies from 0.2 to 0.5 within an increase of the volume fraction. The minimum value of DOLP would allow retrieving the volume fraction of particulate media.
4. *Porosity or structure.* The aggregates or clusters structure formed by different monomers particles play an important role in the spectro-polarimetric light-scattering. Distinct angular light-scattering features are displayed in the backscattering domain (90°–180°). These features vary between the two aggregates and depend on the wavelength.

2.7 Conclusion

Merging spectral and polarimetric light-scattering information is a growing interest in a wide range of scientific fields. Recently, it has been demonstrated how spectral polarimetric light-scattering could be employed to probe microphysical properties of particulate media, for instance mean particle size or relative complex refractive index. This review highlighted the potential use of spectro-polarimetric light-scattering. Fundamental advantages of merging spectral and polarimetric information for light-scattering are to address distinct scattering regimes, probe systems of particles at different scales, and extract useful information about a particulate media of interest. The use of these spectral and polarimetric features for identification of microphysical properties of an unknown particulate media is still recent. Future developments of robust inverse methods remain challenging. The challenge of simultaneous retrieval of microphysical properties of particulate media, without a priori knowledge or use of simplistic assumptions, has been more generally addressed throughout this review.

A comprehensive quantitative analysis of spectro-polarimetric light-scattering by particulate media is presented. In order to perform this quantitative analysis, a broadband hyperspectral and polarimetric scatterometer was developed to measure spectro-polarimetric light-scattering by a large variety of particulate media. For the first time, an experimental set-up has been developed to measure spectro-polarimetric light-scattering by combining a SC laser with a series of hyperspectral and polarimetric sensors. In parallel, different numerical models were developed to compute the spectro-polarimetric light-scattering signatures of particulate media. By solving the spectral VRTE, we have demonstrated that spectral depolarization, or spectral DOP, exhibits significant spectral and polarimetric features relative to a given particulate medium. In a nutshell, the mean particle size has been found to relate to spectral depolarization, the relative complex refractive index to directional depolarization, and the volume fraction to the minimum DOLP value. By solving the DDA for a broadband polarized light, spectral and angular features were proposed to serve as a fingerprint, of sorts, independent of the aggregate's orientation. It may be that such fingerprints contain useful information about the aggregate morphology that would survive orientational averaging. This quantitative analysis, based on experimental and theoretical results, is a first stone for novel optical techniques based on spectro-polarimetric light-scattering to study particulate media.

Acknowledgements The authors would like to thank Matthew Berg for helpful comments regarding radiative transfer equation and for many debates in the field of light-scattering. We are also grateful to Michael I. Mishchenko, Gordon Videen, Ludmilla Kolokolova, and Alex J. Yuffa for fruitful discussions regarding spectral polarimetric light-scattering.

References

Alfano RR, Shapiro SL (1970a) Emission in the region 4000 to 7000 Å via four-photon coupling in glass. Phys Rev Lett 24:584–587. https://doi.org/10.1103/PhysRevLett.24.584

Alfano RR, Shapiro SL (1970b) Observation of self-phase modulation and small-scale filaments in crystals and glasses. Phys Rev Lett 24:592

Althausen D, Müller D, Ansmann A, Wandinger U, Hube H, Clauder E, Zörner S (2000) Scanning 6-wavelength 11-channel aerosol lidar. J Atmos Oceanic Technol 17:1469–1482. https://doi.org/10.1175/1520-0426(2000)017<1469:SWCAL>2.0.CO;2

Ambartsumian VA (1943) Dokl Akad Nauk SSSR 38:257

Ambartsumian VA (1947) Dokl Akad Nauk SSSR 7:199

Ambartsumian VA (1957) Theoretical astrophysics. Translated from the Russian ("Teoreticheskaya astrofizika", Moscow, 1952) by J.B. Sykes, New York: Pergamon Press, 1958, Theoretische Astrophysik - Berlin: Deutscher Verlag der Wissenschaften

Anastasiadou M, Martino AD, Clement D, Liège F, Laude-Boulesteix B, Quang N, Dreyfuss J, Huynh B, Nazac A, Schwartz L, Cohen H (2008) Polarimetric imaging for the diagnosis of cervical cancer. Phys Status Solidi C 5:1423–1426. https://doi.org/10.1002/pssc.200777805

Ångström A (1929) On the atmospheric transmission of sun radiation and on dust in the air. Geogr Ann 11:156–166. https://doi.org/10.2307/519399

Ansmann A, Mattis I, Müller D, Wandinger U, Radlach M, Althausen D, Damoah R (2005) Ice formation in Saharan dust over central Europe observed with temperature/humidity/aerosol Raman lidar. J Geophys Res 110:2. https://doi.org/10.1029/2004JD005000

Arago DFJ (1842) Sur les vulcanes dans la Lune, *Ed. Annuaire de longitudes*, Paris 1929

Arago DFJ (1858) Oeuvres Complètes de François Arago, *Ed.* Gide and J. Baudry, Paris

Asano S, Yamamoto G (1976) Light scattering by a spheroidal particle: errata. Appl Opt 15 (9):2028. https://doi.org/10.1364/AO.15.002028

Aziz T, Firdous S, Khan MA, Ikram M, Rahman TU (2013) Polarimetric study of leukemia human peripheral blood smears in 400–800 nm spectral range. Optik – Int J Light Electron Opt 124 (17):2936–2942. https://doi.org/10.1016/j.ijleo.2012.08.091

Backman V, Harrison GR, Gurjar R, Badizadegan K, Itzkan I (1999) Polarized light scattering spectroscopy for quantitative measurement of epithelial cellular structures in situ. IEEE J Sel Top Quantum Electron 5(4):1019–1026. https://doi.org/10.1109/2944.796325

Banerjee P, Soni J, Purwar H, Ghosh N, Sengupta TK (2013) Probing the fractal pattern and organization of bacillus thuringiensis bacteria colonies growing under different conditions using quantitative spectral light scattering polarimetry. J Biomed Opt 18(3):035003. https://doi.org/10.1117/1.JBO.18.3.035003

Barabashev N (1926) Polarimetrische Beobachtungen an der Mondoberfläche und am Gesteinen. Astron Nachr 229:14–26

Barreda AI, Sanz JM, González F (2015a) Using linear polarization for sensing and sizing dielectric nanoparticles. Opt Express 23(7):9157–9166. https://doi.org/10.1364/OE.23.009157

Barreda AI, Sanz JM, Alcaraz de la Osaa R, Saiza JM, Morenoa F, Gonzáleza F, Videen G (2015b) Using linear polarization to monitor nanoparticle purity. J Quant Spectrosc Radiat Transfer 162:190–196. https://doi.org/10.1016/j.jqsrt.2015.03.005

Bendoula R, Gobrecht A, Moulin B, Roger JM, Bellon Maurel V (2015) Improvement of the chemical content prediction of a model powder system by reducing multiple scattering using polarized light spectroscopy. Appl Spectrosc 69(1):95–102. https://doi.org/10.1366/14-07539

Berdyugina SV, Kuhn JR, Harrington DM, Šantl-Temkiv T, Messersmith EJ (2016) Remote sensing of life: polarimetric signatures of photosynthetic pigments as sensitive biomarkers. Int J Astrobiol 15:45–56. https://doi.org/10.1017/S1473550415000129

Berg MJ (2012) Power-law patterns in electromagnetic scattering: a selected review and recent progress. J Quant Spectrosc Radiat 113(18):2292–2309. https://doi.org/10.1016/j.jqsrt.2012.05.015

Bergstrom RW, Pilewskie P, Russell PB, Redemann J, Bond TC, Quinn PK, Sierau B (2007) Spectral absorption properties of atmospheric aerosols. Atmos Chem Phys 7:5937–5943. https://doi.org/10.5194/acp-7-5937-2007

Boas D, Pitris C, Ramanujam N (2011) Handbook of biomedical, optics. CRC Press, Boca Raton

Boesche E, Stammes P, Ruhtz T, Preusker R, Fischer J (2006) Effect of aerosol microphysical properties on polarization of skylight: sensitivity study and measurements. Appl Opt 45 (34):8790–8805. https://doi.org/10.1364/AO.45.008790

Bohren CF, Huffman DR (1998) Absorption and scattering of light by small particles. Wiley, New York. ISBN 978-0-471-29340-8

Bond TC, Doherty SJ, Fahey DW, Forster PM, Berntsen T, DeAngelo BJ, Flanner MG, Ghan S, Kärcher B, Koch D, Kinne S, Kondo Y, Quinn PK, Sarofim MC, Schultz MG, Schulz M, Venkataraman C, Zhang H, Zhang S, Bellouin N, Guttikunda SK, Hopke PK, Jacobson MZ, Kaiser JW, Klimont Z, Lohmann U, Schwarz JP, Shindell D, Storelvmo T, Warren SG, Zender CS (2013) Bounding the role of black carbon in the climate system: A scientific assessment. J Geophys Res Atmos 118(11):5380–5552. https://doi.org/10.1002/jgrd.50171

Bordier C, Andraud C, Charron E, Lafait J, Anastasiadou M, Martino AD (2008) Illustration of a bimodal system in Intralipid-20% by polarized light scattering: experiments and modeling. Appl Phys A 94(2):347–355. https://doi.org/10.1007/s00339-008-4803-9

Bowell E, Dollfus A, Geake JE (1972) Polarimetric properties of the lunar surface and its interpretation. In: Proceeding Third Lunar Science Conference, vol 3. MIT Press, Cambridge, MA

Box MA, McKellar BHJ (1978) Analytic inversion of multispectral extinction data in the anomalous diffraction approximation. Opt Lett 3(3):91–93. https://doi.org/10.1364/OL.3.000091

Breon FM, Goloub P (1998) Cloud droplet effective radius from spaceborne polarization measurements. Geophys Res Lett 25(11):1879–1882. https://doi.org/10.1029/98GL01221
Brunsting A, Mullaney P (1974) Differential light scattering from spherical mammalian cells. Biophys J 14(6):439–453. https://doi.org/10.1016/S0006-3495(74)85925-4
Bureau (1946) Altimétrie des nuages par impulsions lumineuses, *La météorologie*
Burns WW (1975) Airborne, remote sensing system that uses reflected polarized skylight to detect the presence of oil discharges into water. IEEE Oceans 7:688–692. https://doi.org/10.1109/OCEANS.1975.1154134
Ceolato R, Riviere N (2016) Spectral polarimetric light-scattering by particulate media: 1. Theory of spectral Vector Radiative Transfer. J Quant Spectrosc Radiat 178:117–123. https://doi.org/10.1016/j.jqsrt.2015.12.026
Ceolato R, Riviere N, Hespel L (2012) Reflectances from a supercontinuum laser-based instrument: hyperspectral, polarimetric and angular measurements. Opt Express 20:29413–29425
Ceolato R, Berg MJ, Riviere N (2013) Spectral and angular light-scattering from silica fractal aggregates. J Quant Spectrosc Radiat Transfer 131:160–165. https://doi.org/10.1016/j.jqsrt.2013.01.007
Ceolato R, Golzio M, Riou C, Orlik X, Riviere N (2015) Spectral degree of linear polarization of light from healthy skin and melanoma. Opt Express 23(10):13605–13612. https://doi.org/10.1364/OE.23.013605
Chandrasekhar S (1950) Radiative transfer. Oxford University Press, London
Chen Zh, Sheng P, Weitz DA, Lindsay HM, Lin MY, Meakin P (1988) Optical properties of aggregate clusters. Phys Rev B 37:5232–5235. https://doi.org/10.1103/PhysRevB.37.5232
Chernova G, Kiselev N, Jockers K (1993) Polarimetric characteristic of dust particles as observed in 13 comets: comparisons with asteroids. Icarus 103:144–158. https://doi.org/10.1006/icar.1993.1063
Chwolson OD (1889) Grundzüge einer mathematischen theorie der inneren diffusion des licht. Bull Acad Imp Sci St. Petersburg 33:221–256
Coen S, Chau AHL, Leonhardt R, Harvey JD, Knight JC, Wadsworth WJ, St P, Russell J (2002) Supercontinuum generation by stimulated Raman scattering and parametric four-wave mixing in photonic crystal fibers. J Opt Soc Am B 19:753–764
Coffeen DL (1964) Wavelength dependence of polarization. IV. Volcanic cinders and particles. Astron J 70:403
Corlu A, Choe R, Durduran T, Lee K, Schweiger M, Arridge SR, Hillman EMC, Yodh AG (2005) Diffuse optical tomography with spectral constraints and wavelength optimization. Appl Opt 44(11):2082–2093. https://doi.org/10.1364/AO.44.002082
Corlu A, Choe R, Durduran T, Rosen MA, Schweiger M, Arridge SR, Schnall MD, Yodh AG (2007) Three-dimensional in vivo fluorescence diffuse optical tomography of breast cancer in humans. Opt Express 15(11):6696–6716. https://doi.org/10.4364/OE.15.006696
Cornu A (1890) Sur l'application du photopolarimètre à la météorologie, *Association française pour l'avancement des sciences: conférences de Paris,* compte-rendu de la 19e session, Séance du 11 août 1890
Couch RH, Rowland CW, Ellis KS, Blythe MP, Regan CR, Koch MR, Antill CW, Kitchen WL, Cox JW, DeLorme JF, Crockett SK, Remus RW (1991) Lidar In-Space Technology Experiment (LITE): NASA's first in-space lidar system for atmospheric research. Optical Engineering 30(1):88–95 ISSN 0091-3286
Coulson KL, Dave JV, Sekera Z (1960) Tables related to radiation emerging from a planetary atmosphere with Rayleigh scattering. University of California press, Berkeley
Crovisier J, Leech K, Bockelée-Morvan D, Brooke TY, Hanner MS, Altieri B, Keller HU, Lellouch E (1997) The spectrum of Comet Hale-Bopp (C/1995 O1) observed with the Infrared Space Observatory at 2.9 AU from the Sun. Science 275:1904–1907
Curcio JA, Knestrick GL (1958) Correlation of atmospheric transmission with backscattering. J Opt Soc Am 48(10):686–689. https://doi.org/10.1364/JOSA.48.000686

D'Abzac FX, Kervella M, Hespel L, Dartigalongue T (2012) Experimental and numerical analysis of ballistic and scattered light using femtosecond optical Kerr gating: a way for the characterization of strongly scattering media. Opt Express 20(9):9604–9615
Dehghani H, Pogue BW, Poplack SP, Paulsen KD (2003) Multiwavelength three-dimensional near-infrared tomography of the breast: initial simulation, phantom, and clinical results. Appl Opt 42(1):135–145. https://doi.org/10.1364/AO.42.000135
Deirmendjian D (1964) Scattering and Polarization Properties of Water Clouds and Hazes in the Visible and Infrared. Appl Opt 3(2):187–196. https://doi.org/10.1364/AO.3.000187
Deirmendjian D (1980) A survey of light-scattering techniques used in the remote monitoring of atmospheric aerosols. Rev Geophys Space Phys 18(2):341–360. https://doi.org/10.1029/RG018i002p00341
Del Guasta M, Morandi M, Stefanutti L, Stein B, Wolf JP (1994) Derivation of Mount Pinatubo stratospheric aerosol mean size distribution by means of a multiwavelength lidar. Appl Opt 33 (24):5690–5697. https://doi.org/10.1364/AO.33.005690
Deschamps PY, Breon FM, Leroy M, Podaire A, Bricaud A, Buriez JC, Seze G (2002) The POLDER mission: instrument characteristics and scientific objectives. IEEE Trans Geosci Remote Sens 32(3):598–615. https://doi.org/10.1109/36.297978
Deuzé JL, Herman M, Santer R (1989) Fourier series expansion of the transfer equation in the atmosphere-ocean system. J Quant Spectrosc Radiat Transfer 41(6):483–494
Dial KD, Hiemstra S, Thompson JE (2010) Simultaneous measurement of optical scattering and extinction on dispersed aerosol samples. Anal Chem 82(19):7885–7896
Diner DJ, Xu F, Garay MJ, Martonchik JV, Rheingans BE, Geier S, Davis A, Hancock BR, Jovanovic VM, Bull MA, Capraro K, Chipman RA, McClain SC (2013) The Airborne Multiangle SpectroPolarimetric Imager (AirMSPI): a new tool for aerosol and cloud remote sensing. Atmos Meas Tech 6(2007–2025):2013. https://doi.org/10.5194/amt-6-2007-2013
Ding H, Lu JQ, Brock RS, McConnell TJ, Ojeda JF, Jacobs KM, Hu XH (2007) Angle-resolved Mueller matrix study of light scattering by B-cells at three wavelengths of 442, 633, and 850 nm. J Biomed Opt 12(3):034032. https://doi.org/10.1117/1.2749730
Doicu A, Wriedt T (1999) Calculation of the T-Matrix in the null-field method with discrete sources. J Opt Soc Am A 16(10):2539–2544. https://doi.org/10.1364/JOSAA.16.002539
Dollfus A (1957) Étude des planètes par la polarisation de la lumière. Suppléments aux Annales d'Astrophysique 4:3–114
Dollfus A, Bowell E (1971) Polarimetric properties of the lunar surface and its interpretation. Part. I. Telescopic Obs Astron Astrophys 10:29–53
Draine BT, Flatau PJ (1994) Discrete-dipole approximation for scattering calculations. J Opt Soc Am A 11(4):1491–1499. https://doi.org/10.1364/JOSAA.11.001491
Dreher AW, Reiter K, Weinreb RN (1992) Spatially resolved birefringence of the retinal never fiber layer assessed with a retinal laser ellipsometer. Appl Opt 31(19):3730–3735. https://doi.org/10.1364/AO.31.003730
Dubovik O, Sinyuk A, Lapyonok T, Holben BN, Mishchenko M, Yang P, Eck TF, Volten H, Muñoz O, Veihelmann B, van der Zande WJ, Léon JF, Sorokin M, Slutsker I (2006) The application of spheroid models to account for aerosol particle nonsphericity in remote sensing of desert dust. J Geophys Res 111(D11):D11208. https://doi.org/10.1029/2005JD006619
Dudley J, Genty G, Coen S (2006) Supercontinuum generation in photonic crystal fiber. Rev Mod Phys 78:1135–1184
Eiden R (1966) The elliptical polarization of light scattered by a volume of atmospheric air. Appl Opt 5(4):569–575. https://doi.org/10.1364/AO.5.000569
Ejeta C, Boehnhardt H, Bagnulo S, Tozzi GP (2012) Spectro-polarimetry of the bright side of Saturn's moon. Astron Astrophys 537:A23. https://doi.org/10.1051/0004-6361/201117870
Elias M, Cotte P (2008) Multispectral camera and radiative transfer equation used to depict Leonardo's sfumato in Mona Lisa. Appl Opt 47(12):2146–2154. https://doi.org/10.1364/AO.47.002146
Evans KF, Stephen GL (1991) A new polarized atmospheric radiative transfer model. J Quant Spectrosc Radiat Transfer 46(5):413–423. https://doi.org/10.1016/0022-4073(91)90043-P

Farhoud M (1999) Scattered light from beach sand and its dependence on sand properties. Indian J Pure Appl Phys 37(10):782–786 ISSN:0975-1041

Feingold G, Grund CJ (1994) Feasibility of using multiwavelength lidar measurements to measure cloud condensation nuclei. J Atmos Oceanic Technol 11:1543–1558. https://doi.org/10.1175/1520-0426(1994)011<1543:FOUMLM>2.0.CO;2

Fesenkov VG (1966) On a polarization method to study twilight phenomena. Soviet Astron 43:198

Foitzik L (1965) The spectral extinction of the atmospheric aerosol by Mie particles with different Gaussian distributions, *Gerlands Beitr*. Zur Geophys 74:198–206

Freudenthaler V, Homburg F, Jager H (1996) Optical parameters of contrails from lidar measurements: linear depolarization. Geophys Res Lett 23:3715–3718. https://doi.org/10.1029/96GL03646

Freudenthaler V, Esselborn M, Wiegner M, Heese B, Tesche M, Ansmann A, Müller S, Althausen D, Wirth M, Fix A, Ehret G, Knippertz P, Toledano C, Gasteiger J, Garhammer M, Seefeldner M (2009) Depolarization ratio profiling at several wavelengths in pure Saharan dust during SAMUM 2006. Tellus B 61B(1):165–179. https://doi.org/10.1111/j.1600-0889.2008.00396.x

Ghosh N, Wood MFG, Vitkin IA (2009) Polarimetry in turbid, birefringent, optically active media: a Monte Carlo study of Mueller matrix decomposition in the backscattering geometry. J Appl Phys 105:102023. https://doi.org/10.1063/1.3116129

Ghosh N, Wood MFG, Vitkin IA (2010) Polarized light assessment of complex turbid media such as biological tissues using mueller matrix decomposition. In: Tuchin VV (ed) Handbook of photonics for biomedical science, Chapter 9. CRC Press, Taylor & Francis Group, London, pp 253–282

Ghosh S, Soni J, Purwar H, Jagtap J, Pradhan A, Ghosh N, Panigrahi PK (2011) Differing self-similarity in light scattering spectra: a potential tool for pre-cancer detection. Opt Express 19(20):19717–19730. https://doi.org/10.1364/OE.19.019717

Giakos GC (2006) Multifusion multispectral lightwave polarimetric detection principles and systems. IEEE Trans Instrum Meas 55(6):1904–1912. https://doi.org/10.1109/TIM.2006.884387

Gobbi GP, Barnaba F, Giorgi R, Santacasa A (2000) Altitude–resolved properties of a Saharan dust event over the Mediterranean. Atmos Environ 34:5119–5127

Goldstein DH, Chenault DB (2002) Spectropolarimetric reflectometer. Opt Eng 41(05):1013–1020. https://doi.org/10.1117/1.1467933

Goloub P, Deuze JL, Herman M, Fouquart Y (1994) Analysis of the POLDER airborne polarization measurements performed over cloud covers. IEEE Trans Geosci Remote Sens 32:78–87. https://doi.org/10.1109/36.285191

Gouesbet G, Gréhan G (2011) Generalized Lorenz-Mie theories. Springer Science & Business Media, Berlin. ISBN ISBN 364217194X, 9783642171949

Gramm GW, Blifford IH Jr, Gillette DA, Russel PB (1974a) Complex index of refraction of airborne soil particles. J Appl Meteorol 13:459–471. https://doi.org/10.1175/1520-0450(1974)013<0459:CIOROA>2.0.CO;2

Gramm GW, Blifford IH, Gillette DA, Russell PB (1974b) Complex index of refraction of airborne soil particles. J Appl Meteorol 6282:459–471. https://doi.org/10.1175/1520-0450(1974)013<0459:CIOROA>2.0.CO;2

Grassl H (1971) Determination of aerosol size distributions from spectral attenuation measurements. Appl Opt 10(11):2534–2538. https://doi.org/10.1364/AO.10.002534

Gross CT, Salamon H, Hunt AJ, Macey RI, Orme F, Quintanilha AT (1991) Hemoglobin polymerization in sickle cells studied by circular polarized light scattering. Biochem Biophys Acta 1079(2):152–160. https://doi.org/10.1016/0167-4838(91)90120-O

Groß S, Tesche M, Freudenthaler V, Toledano C, Wiegner M, Ansmann A, Althausen D, Seefeldner M (2011) Characterization of Saharan dust, marine aerosols and mixtures of biomass-burning aerosols and dust by means of multi-wavelength depolarization and Raman lidar measurements during SAMUM 2. Tellus B 63B(4):706–724. https://doi.org/10.1111/j.1600-0889.2011.00556.x

Gurjar RS, Backman V, Perelman LT, Georgakoudi I, Badizadegan K, Itzkan I, Dasari RR, Feld MS (2001) Imaging human epithelial properties with polarized light scattering spectroscopy. Nat Med 7(11):1245–1248. https://doi.org/10.1038/nm1101-1245

Gustafson Bo ÅS, Kolokolova L (1999) A systematic study of light scattering by aggregate particles using the microwave analog technique: Angular and wavelength dependence of intensity and polarization. J Geophys Res 104(D24):31711–31720. https://doi.org/10.1029/1999JD900327

Hadamard J (1902) Sur les problèmes aux dérivées partielles et leur signification physique. Princeton Univ Bull 13:49–52

Hage J, Greenberg J, Wang R (1991) Scattering from arbitrarily shaped particles: theory and experiment. Appl Opt 30(9):1141–1152. https://doi.org/10.1364/AO.30.001141

Hakala T, Suomalainen J, Kaasalainen S, Chen Y (2012) Full waveform hyperspectral LiDAR for terrestrial laser scanning. Opt Express 20:7119–7127

Hariharan TA, Sekera Z (1966) A photoelectric skylight polarimeter. Appl Opt 5(9):1415–1417. https://doi.org/10.1364/AO.5.001415

Hastings FD, Schneider JB (1995) A Monte-Carlo FDTD technique for rough surface scattering. IEEE Trans Antennas Propag 43(11):1183–1191

Hayashida S, Kobayashi A, Iswasaka Y (1984) Lidar measurements of stratospheric aerosol content and depolarization ratios after the eruption of El Chichon volcano: measurements at Nagoya. Japan. Geofisica Int 23(2):277–288 ISSN:0016-7169

`Heintzenberg J, Müller H, Quenzel H, Thomalla E (1981) Information content of optical data with respect to aerosol properties: numerical studies with a randomized minimization-search-technique inversion algorithm. Appl Opt 20(8):1308–1315. https://doi.org/10.1364/AO.20.001308

Hespel L, Delfour A (2000) Mie light-scattering granulometer with adaptive numerical filtering. I. Theory Appl Opt 39:6897–6917

Holben BN, Eck TF, Slutsker I, Tanré D, Buis JP, Setzer A, Vermote E, Reagan JA, Kaufman YJ, Nakajima T, Lavenu F, Jankowiak I, Smirnov A (1998) AERONET—A federated instrument network and data archive for aerosol characterization. Remote Sensing of Environment 66 (1):1–16. https://doi.org/10.1016/S0034-4257(98)00031-5 ISSN:0034-4257

Holland AC, Gagne G (1970) The scattering of polarized light by polydisperse systems of irregular particles. Appl Opt 9(5):1113–1121. https://doi.org/10.1364/AO.9.001113

Hollstein A, Ruhtz T, Fischer J, Preusker R (2009) Optimization of system parameters for a complete multispectral polarimeter. Appl Opt 48(24):4767–4773. https://doi.org/10.1364/AO.48.004767

Hovenier JW (1971) Multiple scattering of polarized light in planetary atmospheres. Astron Astrophys 13:7

Huckaby JL, Ray AK, Das B (1994) Determination of size, refractive index, and dispersion of single droplets from wavelength-dependent scattering spectra. Appl Opt 33(30):7112–7125. https://doi.org/10.1364/AO.33.007112

Ientilucci E, Gartley M (2009) Impact of BRDF on physics-based modeling as applied to target detection in hyperspectral imagery. In: Proceeding SPIE 7334, 73340T1

Ishimaru A, Lesselier D, Yeh C (1984) Multiple scattering calculations for nonspherical particles based on the vector radiative transfer theory. Radio Sci 19(5):1356–1366. https://doi.org/10.1029/RS019i005p01356

Jagodnicka AK, Stacewicz T, Karasiński G, Posyniak M, Malinowski SP (2009) Particle size distribution retrieval from multiwavelength lidar signals for droplet aerosol. Appl Opt 48:B8–B16. https://doi.org/10.1364/AO.48.0000B8

Janzen J (1979) The refractive index of colloidal carbon. J Colloid Interface 69:436–447

Jeffrey DJ, Acrivos A (1976) The rheological properties of suspensions of rigid particles. AIChE J 22:417–432

Johnson EA, Meyer RC, Hopkins RE, Mock WH (1939) The measurements of light scattered by the upper atmosphere from a search-light beam. J Opt Soc Am 29(12):512–517. https://doi.org/10.1364/JOSA.29.000512

Johnson B, Joseph R, Nischan ML, Newbury AB, Kerekes JP, Barclay HT, Willard BC, Zayhowski JJ (1999) Compact active hyperspectral imaging system for the detection of concealed targets. In: Proceeding SPIE 3710, Detection and remediation technologies for mines and mine like targets iv. https://doi.org/10.1117/12.357002

Johnston RG, Singham SB, Salzman GC (1988) Polarized light scattering. Comments Mo Cell Biophys 5(3):171–192

Jones RC (1941) New calculus for the treatment of optical systems. J Opt Soc Am 31(7):488–493. https://doi.org/10.1364/JOSA.31.000488

Kalashnikova OV, Sokolik IN (2004) Modeling the radiative properties of nonspherical soil-derived mineral aerosols. J Quant Spectrosc Radiat Transfer 87(2):137–166. https://doi.org/10.1016/j.jqsrt.2003.12.026

Khlebstov NG (2001) Orientational averaging of integrated cross sections in the discrete dipole method. Opt Spectrosc 90(3):408–415. https://doi.org/10.1134/1.1358452

Kim A, Moscoso M (2001) Influence of the relative refractive index on the depolarization of multiply scattered waves. Phys Rev E 64:026612

Kimura H, Kolokolova L, Mann I (2003) Optical properties of cometary dus-Constraints from numerical studies on light scattering by aggregate particles. Astron Astrophys 407:L5–L8

King MD, Byrne DM, Herman BM, Reagan JA (1978) Aerosol size distributions obtained by inversions of spectral optical depth measurements. J Atmos Sci 35(11):2153–2167

Kiselev NN, Jockers K, Rosenbush V, Velichko F, Bonev T, Karpov N (2000) Anomalous wavelength dependence of polarization of Comet 21P/Giacobini-Zinner. Planet Space Sci 48:1005–1009

Klett JD (1981) Stable analytic inversion solution for processing lidar returns. Appl Opt 20 (2):211–220. https://doi.org/10.1364/AO.20.000211

Klett JD (1984) Anomalous diffraction model for inversion of multispectral extinction data including absorption effects. Appl Opt 23(24):4499–4508. https://doi.org/10.1364/AO.23.004499

Kolokolova L (2016) Cometary dust under the microscope. Nature 537:37–38. https://doi.org/10.1038/537037a

Kolokolova L, Jockers K (1997) Composition of cometary dust from polarization spectra. Planet Space Sci 45:1543–1550

Kolokolova L, Kimura H (2010) Effects of electromagnetic interaction in the polarization of light scattered by cometary and other types of cosmic dust. Astron Astrophys 513:A40. https://doi.org/10.1051/0004-6361/200913681

Kuik F, Stammes P, Hovenier JW (1991) Experimental determination of scattering matrices of water droplets and quartz particles. Appl Opt 30(33):4872–4881. https://doi.org/10.1364/AO.30.004872

Lambert-Girard S, Hô N, Bourliaguet B, Paradis P-F, Piché M, Babin F (2012) Proposal for a standoff bio-agent detection SWIR/MWIR differential scattering lidar. In: Proceeding SPIE 8358, Chemical, Biological, Radiological, Nuclear, and Explosives (CBRNE) Sensing XIII, vol 835805. https://doi.org/10.1117/12.918680

Landau LD, Lifshitz EM (1960) Electrodynamics of continuous media. Pergamon, Oxford

Lang-Yona N, Rudich Y, Segre E, Dinar E, Abo-Riziq A (2009) Complex refractive indices of aerosols retrieved by continuous wave-cavity ring down aerosol spectrometer. Anal Chem 81 (5):1762–1769

Larusson F, Fantini S, Miller EL (2011a) Hyperspectral image reconstruction for diffuse optical tomography. Biomed Opt Express 2(4):46–965. https://doi.org/10.1364/BOE.2.000946

Larusson F, Fantini S, Miller EL (2011b) Hyperspectral image reconstruction for diffuse optical tomography. Biomed Opt Express 2(4):946–965. https://doi.org/10.1364/BOE.2.000946

Le Borgne JF, Crovisier JL, Arnaud J (1987) Polarimetry of visible and near UV molecular bands: Comets P/Halley and Hartley-Good. Astron Astrophys 173:180–182

Le Hors L, Hartemann P, Breugnot S (2000) Multispectral polarization active imager in the visible band. In: Proceeding SPIE 4035, Laser radar technology and applications V, vol 380. https://doi.org/10.1117/12.397809

Lee RL, Samudio OR (2012) Spectral polarization of clear and hazy coastal skies. Appl Opt 51(31):7499–7508. https://doi.org/10.1364/AO.51.007499

Lenham AP, Clay MR (1982) Drop-size distribution of fog droplets determined from transmission measurements in the 0.53–10.1 μm. Appl Opt 21(23):4191–4193. https://doi.org/10.1364/AO.21.004191

Li D, Zeng N, Zeng M, Liao R, Ma H (2015) Identification of soot particles in air using polarization scattering method. In: Proceeding SPIE 9613, Polarization science and remote sensing VII, 961315. https://doi.org/10.1117/12.2193211

Ligon DA, Gillespie JB, Pellegrino P (2000) Aerosol properties from spectral extinction and backscatter estimated by an inverse Monte Carlo method. Appl Opt 39(24):4402–4410. https://doi.org/10.1364/AO.39.004402

Liu Y, Arnott WP, Hallett J (1999) Particle size distribution retrieval from multispectral optical depth: influences of particle nonsphericity and refractive index. J Geophys Res 104 (D24):31753–31762. https://doi.org/10.1029/1998JD200122

Liu L, Mishchenko MI, Arnott WP (2008) A study of radiative properties of fractal soot aggregates using the superposition T-Matrix method. J Quant Spectrosc Radiat Transfer 109(15):2656–2663. https://doi.org/10.1016/j.jqsrt.2008.05.001

Lommel E (1889) Die Photometrie der diffusen Zuruckwerfung. Ann Phys 272:473–502

Lorenz LV (1890) Upon the light reflected and refracted by a transparent sphere. Vidensk Selsk Skrifter 6:1–62

Lyot B (1929) Recherches sur la polarisation de la lumière des planètes et de quelques substances terrestres. Ann Obs Meudon 8(1):1–161

Ma X, Lu JQ, Brock RS, Jacobs KM, Yang P, Hu XH (2003) Determination of complex refractive index of polystyrene microspheres from 370 to 1610 nm. Phys Med Biol 48(24):4165–4172

Mackowski DW (2002) Discrete dipole moment method for calculation of the T-matrix for nonspherical particles. J Opt Soc Am A 19(5):881–893. https://doi.org/10.1364/JOSAA.19.000881

Mackowski DW, Mishchenko MI (1996) Calculation of the T-Matrix and the scattering matrix for ensembles of spheres. J Opt Soc Am A 11(13):2266–2278. https://doi.org/10.1364/JOSAA.13.002266

Manninen A, Kääriäinen T, Parviainen T, Buchter S, Heiliö M, Laurila T (2014) Long distance active hyperspectral sensing using high-power near-infrared supercontinuum light source. Opt Express 22(6):7172–7177. https://doi.org/10.1364/OE.22.007172

Manolakis D, Marden D (2003) Hyperspectral image processing for automatic target detection applications. Lincoln Lab J 14:79–116

Markel VA, Muratov L, Stockman M, George T (1991) Theory and numerical simulation of optical properties of fractal clusters. Phys Rev B 43(10):8183–8195. https://doi.org/10.1103/PhysRevB.43.8183

Maxwell JC (1865) A dynamical theory of the electromagnetic field. Philos Trans R Soc Lond 155:459–512

McCord TB (1969) Color differences on the lunar surface. J Geophys Res 74(12):3131–3142

McCord TB, Charette MP, Johnson TV, Lebofsky LA, Pieters C, Adams JB (1972) Lunar spectral types. J Geophys Res 77(8):1349–1359. https://doi.org/10.1029/JB077i008p01349

McNeil WR, Carswell AI (1975) Lidar polarization studies of the troposphere. Appl Opt 14 (9):2158–2168. https://doi.org/10.1364/AO.14.002158

Méjean G, Kasparian J, Salmon E, Yu J, Wolf J-P, Bourayou R, Sauerbrey R, Rodriguez M, Wöste L, Lehmann H, Stecklum B, Laux U, Eislöffel J, Scholz A, HatzesMejan AP (2003) Towards a supercontinuum-based infrared lidar. Appl Phys B 77(2):357–359. https://doi.org/10.1007/s00340-003-1183-x

Mie G (1908) Beiträge zur Optiktrüber Medien speziell kolloidaler Metallösungen. Ann Phys 330:3

Milham ME, Frickel RH, Embury JF, Anderson DH (1981) Determination of optical constants from extinction measurements. J Opt Soc Am 71(9):1099–1106. https://doi.org/10.1364/JOSA.71.001099

Mishchenko MI (2011) Directional radiometry and radiative transfer: A new paradigm. J Quant Spectrosc Radiat 112:2079–2094. https://doi.org/10.1016/j.jqsrt.2011.04.006

Mishchenko MI, Sassen K (1998) Depolarization of lidar returns by small ice crystals: an application to contrails. Geophys Res Lett 25(3):309–312. https://doi.org/10.1029/97GL03764

Mishchenko MI, Yurkin MA (2017) On the concept of random orientation in far-field electromagnetic scattering by nonspherical particles. Opt Lett 42(3):494–497. https://doi.org/10.1364/OL.42.000494

Mishchenko MI, Mackowski DW, Travis LD (1995) Scattering of light by bispheres with touching and separated components. Appl Opt 34(21):4589–4599. https://doi.org/10.1364/AO.34.004589

Mishchenko MI, Travis LD, Kahn RA, West RA (1997) Modeling phase functions for dustlike tropospheric aerosols using a shape mixture of randomly oriented polydisperse spheroids. J Geophys Res 102(D14):16831–16847. https://doi.org/10.1029/96JD02110

Mishchenko MI, Hovenier JW, Travis LD (2000) Light scattering by nonspherical particles: theory, measurements, and applications. Academic Press, San Diego

Mishchenko MI, Travis LD, Lacis AA (2002) Scattering, absorption, and emission of light by small particles. Cambridge University Press, Cambridge

Mishchenko MI, Travis LD, Lacis AA (2006) Multiple scattering of light by particles. Cambridge University Press, Cambridge

Mohanty SK, Ghosh N, Majumder SK, Gupta PK (2001) Depolarization of autofluorescence from malignant and normal human breast tissues. Appl Opt 40(7):1147–1154. https://doi.org/10.1364/AO.40.001147

Moorthy KK, Nair PR, Krishna Murthy BV (1991) Size distribution of coastal aerosols: effects of local sources and sinks. J Appl Meteorol 30(6):844–852. https://doi.org/10.1175/1520-0450(1991)030<0844:SDOCAE>2.0.CO;2

Mourant J, Freyer J, Heilscher A, Eick A, Shen D, Johnson T (1998) Mechanisms of light scattering from biological cells relevant to non-invasive optical-tissue diagnosis. Appl Opt 37(16):3586–3593. https://doi.org/10.1364/AO.37.003586

Mourant JR, Johnson TM, Carpenter S, Guerra A, Aida T, Freyer JP (2002) Polarized angular dependent spectroscopy of epithelial cells and epithelial cell nuclei to determine the size scale of scattering structures. J Biomed Opt 7(3):378–387. https://doi.org/10.1117/1.1483317

Mudd HT, Kruger CH, Murray ER (1982) Measurement of IR laser backscatter spectra from sulfuric acid and ammonium sulfate aerosols. Appl Opt 21(6):1146–1154. https://doi.org/10.1364/AO.21.001146

Mueller H (1943) Memorandumon the polarization optics of the photo-elastic shutter. In: Project OEMsr-576

Muller H, Quenzel H (1985) Information content of multispectral lidar measurements with respect to the aerosol size distribution. Appl Opt 24(5):648–654. https://doi.org/10.1364/AO.24.000648

Müller D, Wandinger U, Althausen D, Mattis I, Ansmann A (1998) Retrieval of physical particle properties from lidar observations of extinction and backscatter at multiple wavelengths. Appl Opt 37(12):2260–2263. https://doi.org/10.1364/AO.37.002260

Müller D, Wandinger U, Ansmann A (1999) Microphysical particle parameters from extinction and backscatter lidar data by inversion with regularization: theory. Appl Opt 38(12):2346–2357. https://doi.org/10.1364/AO.38.002346

Müller D, Wagner F, Wandinger U, Ansmann A, Wendisch M, Althausen D, von Hoyningen-Huene W (2000) Microphysical particle parameters from extinction and backscatter lidar data by inversion with regularization: experiment. Appl Opt 39(12):1879–1892. https://doi.org/10.1364/AO.39.001879

Müller D, Veselovskii I, Kolgotin A, Tesche M, Ansmann A, Dubovik O (2013) Vertical profiles of pure dust and mixed smoke–dust plumes inferred from inversion of multiwavelength Raman/polarization lidar data and comparison to AERONET retrievals and in situ observations. Appl Opt 52:3178–3202. https://doi.org/10.1364/AO.52.003178

Munoz O, Hovenier JW (2011) Laboratory measurements of single light scattering by ensembles of randomly oriented small irregular particles in air. J Quant Spectrosc Radiat Transfer 112:1646–1657. https://doi.org/10.1016/j.jqsrt.2011.02.005

Muñoz O, Volten H, de Haan JF, Vassen W, Hovenier JW (2000) Experimental determination of scattering matrices of olivine and Allende meteorite particles. Astron Astrophys 360:777–788

Murayama T, Furushima M, Oda A, Iwasaka N, Kai K (1996) Depolarization ratio measurements in the atmospheric boundary layer by lidar in Tokyo. J Meteorol Soc Jpn 74(4):571–578 ISSN:0026-1165

Myers R, Nordsieck K (1984) Spectropolarimetry of comets Austin and Churyumov-Gerasimenko. Icarus 58:431–439. https://doi.org/10.1016/0019-1035(84)90088-5

Nagdimunov L (2013) Polarimetric technique to study (pre)biological organics in cosmic dust and planetary aerosols. Earth Planets Space 65:14

Nilsson B (1979) Meteorological influence on aerosol extinction in the 0.2–40 μm wavelength range. Appl Opt 18(20):3457–3473. https://doi.org/10.1364/AO.18.003457

Novikova T, Pierangelo A, Manhas S, Benali A, Validire P, Gayet B, De Martino A (2014) The origins of polarimetric image contrast between healthy and cancerous human colon tissue. Appl Phys Lett 102:241103. https://doi.org/10.1063/1.4811414

Okada K, Heintzenberg J, Kai K, Qin Y (2001) Shape of atmospheric mineral particles collected in three Chinese arid-regions. Geophys Res Lett 28(16):3123. https://doi.org/10.1029/2000GL012798

Olsen RO, Okrasinski R, Ben-Shalom A (1983) Measured spectral extinction coefficient dependence of vehicle dust at visible, infrared and near-millimeter wavelengths. Infrared Phys 23(6):301–306. https://doi.org/10.1016/0020-0891(83)90002-7

Pathria RK (2003) Statistical mechanics, 2nd edn. Butterworth Heinemann, Oxford

Patskovsky S, Bergeron E, Rioux D, Simarda M, Meuniera M (2014) Hyperspectral reflected light microscopy of plasmonic Au/Ag alloy nanoparticles incubated as multiplex chromatic biomarkers with cancer cells. Analyst 139:5247–5253

Peng Y, Lu R (2008) Analysis of spatially resolved hyperspectral scattering images for assessing apple fruit firmness and soluble solids content. Postharvest Biol Technol 48:52–62

Perelman LT, Backman V, Wallace M, Zonios G, Manoharan R, Nusrat A, Shields S, Seiler M, Lima C, Hamano T, Itzkan I, Van Dam J, Crawford JM, Feld MS (1998) Observation of periodic fine structure in reflectance from biological tissue: a new technique for measuring nuclear size distribution. Phys Rev Lett 80(3):627–630. https://doi.org/10.1103/PhysRevLett.80.627

Pieters CM (1999) The Moon as a spectral calibration standard enabled by lunar samples: the Clementine example in new views of the Moon II, Workshop, vol **8025**

Pilbratt GL, Riedinger JR, Passvogel T, Crone G, Doyle D, Gageur U, Heras AM, Jewell C, Metcalfe L, Ott S, Schmidt M (2010) Herschel Space Observatory, an ESA facility for far-infrared and submillimetre astronomy. Astron Astrophys 518:L1. https://doi.org/10.1051/0004-6361/201014759

Pospergelis MM (1969) Spectroscopic measurements of the four Stokes parameters for light scattered by natural objects. Sov Astron 12:973–977

Post MJ, Grund CJ, Langford AO, Proffitt MH (1992) Observations of Pinatubo ejecta over Boulder, Colorado by lidars of three different wavelengths. Geophys Res Lett 19:195–198. https://doi.org/10.1029/91GL02794

Powers MA, Davis CC (2012) Spectral LADAR: active range-resolved three-dimensional imaging spectroscopy. Appl Opt 51(10):1468–1478. https://doi.org/10.1364/AO.51.001468

Pritchard BS, Elliott WG (1960) Two instruments for atmospheric optics measurements. J Opt Soc Am 50(3):191–202. https://doi.org/10.1364/JOSA.50.000191

Purcell EM, Pennypacker CR (1973) Scattering and absorption of light by nonspherical dielectric grains. Astrophys J 186:705–714. https://doi.org/10.1086/152538

Pyaskovskaya-Fesenkova EV (1958) On scattering and polarization of light in desert conditions. Dokl Akad Nauk SSSR 123(6):1006–1009

Qi J, Barrière C, Wood TC, Elson DS (2012) Polarized multispectral imaging in a rigid endoscope based on elastic light scattering spectroscopy. Biomed Opt Express 3(9):2087–2099. https://doi.org/10.1364/BOE.3.002087

Qing P, Nakane H, Sasano Y, Kitamura S (1989) Numerical simulation of the retrieval of aerosol size distribution from multiwavelength laser radar measurements. Appl Opt 28(24):5259–5265. https://doi.org/10.1364/AO.28.005259

Rajeev K, Parameswaran K (1998) Iterative method for the inversion of multiwavelength lidar signals to determine aerosol size distribution. Appl Opt 37(21):4690–4700. https://doi.org/10.1364/AO.37.004690

Ramella-Roman JC, Nayak A, Prahl SA (2011) Spectroscopic sensitive polarimeter for biomedical applications. J Biomed Opt 16(4):047001. https://doi.org/10.1117/1.3561907

Ranka JK, Windeler RS, Stentz AJ (2000) Visible continuum generation in air–silica microstructure optical fibers with anomalous dispersion at 800 nm. Opt Lett 25:25–27

Ray A, Kopelman R, Chon B, Briggman K, Hwang J (2016) Scattering based hyperspectral imaging of plasmonic nanoplate clusters towards biomedical applications. J Biophotonics 9:721–729

Reichardt J, Tsias A, Behrendt A (2000) Optical properties of PSC Ia-enhanced at UV and visible wavelengths: model and observations. Geophys Res Lett 27:201–204. https://doi.org/10.1029/1999GL010904

Richardson JM, Aldridge JC, Milstein AB (2008) Polarimetric lidar signatures for remote detection of biological warfare agents. In: Proceeding SPIE 6972, Polarization: measurement, analysis, and remote sensing VIII, 69720E. https://doi.org/10.1117/12.777833

Richert M, Orlik X, de Martino A (2009) Adapted polarization state contrast image. Opt Express 17(16):14199–14210. https://doi.org/10.1364/OE.17.014199

Riviere N, Ceolato R, Hespel L (2012) Multispectral polarized BRDF: design of a highly resolved reflectometer and development of a data inversion technique. Optica Applicata 42:7–22

Riviere N, Ceolato R, Hespel L (2013) Polarimetric and angular light-scattering from dense media: comparison of a vectorial radiative transfer model with analytical, stochastic and experimental approaches. J Quant Spectrosc Radiat Transfer 131:88–94. https://doi.org/10.1016/j.jqsrt.2013.04.019

Roslund C, Beckman C (1994) Disputing Viking navigation by polarized light. Appl Opt 33(21):4754–4755. https://doi.org/10.1364/AO.33.004754

Rozenberg GV (1968) Optical investigations of atmospheric aerosols. Sov Phys Usp 11(3):353–380

Sakai T, Nagai T, Kobayashi T, Yamazaki A, Uchiyama A, Mano Y (2007) Multiwavelength and polarization lidar measurements of Asian dust layers over Tsukuba, Japan: a case study. Atmos Chem Phys Discuss 7(4):10179–10203. https://doi.org/10.5194/acpd-7-10179-2007

Sasano Y, Browell EV (1989) Light scattering characteristics of various aerosol types derived from multiple wavelength lidar observations. Appl Opt 28(9):1670–1679. https://doi.org/10.1364/AO.28.001670

Sassen K (1991) The polarization lidar technique for cloud research: a review and current assessment. Bull Am Meteor Soc 72:1848–1866. https://doi.org/10.1175/1520-0477(1991)072<1848:TPLTFC>2.0.CO;2

Sassen K, Zhu J, Webley P, Dean K, Cobb P (2007) Volcanic ash plume identification using polarization lidar: Augustine eruption, Alaska. Geophys Res Lett 34:L08803. https://doi.org/10.1029/2006GL027237

Scheffold F, Cerbino R (2007) New trends in light scattering. Curr Opin Colloid Interface Sci 12(1):50–57. https://doi.org/10.1016/j.cocis.2007.03.005

Schotland RM, Sassen K, Stone R (1971) Observations by lidar of linear depolarization ratios for hydrometeors. J Appl Meteorol 10:1011–1017. https://doi.org/10.1175/1520-0450(1971)010<1011:OBLOLD>2.0.CO;2

Schuster A (1905) Radiation through a foggy atmosphere. Astrophys J 21:1. https://doi.org/10.1086/141186

Sekera Z (1957) Light scattering in the atmosphere and the polarization of sky light. J Opt Soc Am 47(6):484–490. https://doi.org/10.1364/JOSA.47.000484

Sellmeier W (1871) Zur Erklärung der abnormen Farbenfolge im Spectrum einiger Substanzen. Ann der Phys und Chem 219

Sharma N, Arnold IJ, Moosmüller H, Arnott WP, Mazzoleni C (2013) Photoacoustic and nephelometric spectroscopy of aerosol optical properties with a supercontinuum light source. Atmos Meas Tech 6:3501–3513. https://doi.org/10.5194/amt-6-3501-2013

Shaw GE, Reagan JA, Herman BM (1973a) Investigations of atmospheric extinction using direct solar radiation measurements made with multiple wavelength radiometer. J Appl Meteorol 12(2):374–380. https://doi.org/10.1175/1520-0450(1973)012<0374:IOAEUD>2.0.CO;2

Shaw GE, Reagan JA, Herman BM (1973b) Investigations of atmospheric extinction using direct solar radiation measurements made with multiple wavelength radiometer. J Appl Meteorol 12:374

Shkuratov YG (1980) Albedo of asteroids. Sov Astron J 57(6):1320–1322

Shkuratov YG (1981) Connection between the albedo and polarization properties of the Moon. Fresnel component of reflected light. Sov Astron J 25:490

Shkuratov YG, Muinonen K, Bowell E, Lumme K, Peltoniemi J, Kreslavsky MA, Stankevich DG, Tishkovetz VP, Opanasenko NV, Malkumova LY (1994) A critical review of theoretical models of negatively polarized light scattered by atmosphereless solar system bodies. Earth Moon Planet 65:201–246

Sokolov K (1999) Reflectance spectroscopy with polarized light: is it sensitive to cellular and nuclear morphology. Opt Express 5(13):302–317. https://doi.org/10.1364/OE.5.000302

Soni J, Jose GP, Ghosh S, Pradhan A, Sengupta TK, Panigrahi PK, Ghosh N (2011) Probing tissue multifractality using wavelet based multifractal detrended fluctuation analysis: applications in precancer detection. In: 4th International Conference on Biomedical Engineering and Informatics (BMEI), vol 1, pp 448–452. https://doi.org/10.1109/BMEI.2011.6098255

Sorensen CM, Cai J, Lu N (1992) Light-scattering measurements of monomer size, monomers per aggregate, and fractal dimension for soot aggregates in flames. Appl Opt 31(30):6547–6557. https://doi.org/10.1364/AO.31.006547

Sparks WB, Hough J, Germer TA, Chen F, DasSarma S, DasSarma P, Robb FT, Manset N, Kolokolova L, Reid N, Macchetto FD, Martin W (2009) Detection of circular polarization in light scattered from photosynthetic microbes. Proc Natl Acad Sci USA 106(19):7816–7821. https://doi.org/10.1073/pnas.0810215106

Stenflo JO, Biverot H, Stenmark L (1976) Ultraviolet polarimeter to record resonance-line polarization in the solar spectrum around 130–150 nm. Appl Opt 15:1188–1198. https://doi.org/10.1364/AO.15.001188

Sterzik MF, Palle SBE (2012) Biosignatures as revealed by spectropolarimetry of Earthshine. Nature 483:64–66

Stokes GC (1852) On the composition and resolution of streams of polarized light from different sources. Trans Cambridge Philos Soc 9:399–416

Stowe LL (1977) Polarization of reflected sunlight as measured from a high-altitude balloon. In: Proceeding SPIE 0112, optical polarimetry: instrumentation and applications, pp 176–183. https://doi.org/10.1117/12.955561

Sugimoto N, Lee CH (2006) Characteristics of dust aerosols inferred from lidar depolarization measurements at two wavelengths. Appl Opt 45(28):7468–7474. https://doi.org/10.1364/AO.45.007468

Sugimoto N, Matsui I, Shimizu A, Uno I, Asai K (2002) Observation of dust and anthropogenic aerosol plumes in the Northwest Pacific with a two-wavelength polarization lidar on board the research vessel Mirai. Geophys Res Lett 29(19). https://doi.org/10.1029/2002GL015112

Sun W, Pan H, Videen G (2009) General finite-difference time-domain solution of an arbitrary electromagnetic source interaction with an arbitrary dielectric surface. Appl Opt 48:6015–6025. https://doi.org/10.1364/AO.48.006015

Sun W, Videen G, Lin B, Hu Y, Fu Q (2011) Beyond Snell's law: refraction of a nano-beam of light. J Quant Spectrosc Radiat 112:174–176. https://doi.org/10.1016/j.jqsrt.2010.03.009

Sun W, Videen G, Fu Q, Hu Y (2013a) Scattered-field FDTD and PSTD algorithms with CPML absorbing boundary conditions for light scattering by aerosols. J Quant Spectrosc Radiat 131:166–174. https://doi.org/10.1016/j.jqsrt.2013.07.015

Sun W, Liu Z, Videen G, Fu Q, Muinonen K, Winker DM, Lukashin C, Jin Z, Lin B, Huang J (2013b) For the depolarization of linearly polarized light by smoke particles. J Quant Spectrosc Radiat 122:233–237. https://doi.org/10.1016/j.jqsrt.2012.03.031

Sun Z, Zhang J, Zhao Y (2013c) Laboratory studies of polarized light reflection from sea ice and lake ice in visible and near infrared. IEEE Geosci Remote Sens Lett 10:170–173

Sun W, Videen G, Mishchenko MI (2014a) Detecting super-thin clouds with polarized sunlight. Geophys Res Lett 41:688–693. https://doi.org/10.1002/2013GL058840

Sun Z, Zhang J, Tong Z, Zhao Y (2014b) Particle size effects on the reflectance and negative polarization of light backscattered from natural surface particulate. J Quant Spectrosc Radiat Transfer 133:1–12. https://doi.org/10.1016/j.jqsrt.2013.03.013

Sun W, Lukashin C, Baize RR, Goldin D (2015a) Modeling polarized solar radiation for CLARREO inter-calibration applications: validation with PARASOL data. J Quant Spectrosc Radiat Transfer 150:121–133. https://doi.org/10.1016/j.jqsrt.2014.05.013

Sun W, Baize RR, Lukashin C, Videen G, Hu Y, Lin B (2015b) Modeling polarized solar radiation of the ocean-atmosphere system for satellite remote sensing applications, light scattering reviews. Praxis Publishing, United Kingdom, p 10

Suzuki T, Kurosaki H, Enkyo S, Koshiishi H (1997) Application of an AOTF imaging spectro-polarimeter. In: Proceeding SPIE 3121, polarization: measurement, analysis, and remote sensing. https://doi.org/10.1117/12.278978

Swami M, Manhas S, Patel H, Gupta P (2010) Mueller matrix measurements on absorbing turbid medium. Appl Opt 49(18):3458–3464. https://doi.org/10.1364/AO.49.003458

Tanaka M, Nakajima T, Takamura T (1982) Simultaneous determination of the complex refractive index and size distribution of airborne and water suspended particles from light scattering measurements. J Meteorol Soc Jpn 60(6):1259–1272

Tang C, Aydin K (1995) Scattering from ice crystals at 94 and 220 GHz millimetre wave frequencies. IEEE Trans Geosci Remote Sens GE-33:93–99

Tang H, Lin JZ (2013) Retrieval of spheroid particle size distribution from spectral extinction data in the independent mode using PCA approach. J Quant Spectrosc Radiat Transfer 115:78–92. https://doi.org/10.1016/j.jqsrt.2012.09.005

Thompson RC, Bottiger JR, Fry ES (1980) Measurement of polarized light interactions via the Mueller matrix. Appl Opt 19(8):1323–1332. https://doi.org/10.1364/AO.19.001323

Tishkovets VP, Petrova EV, Jockers K (2004) Optical properties of aggregate particles comparable in size to the wavelength. J Quant Spectrosc Radiat Transfer 86(3):241–265. https://doi.org/10.1016/j.jqsrt.2003.08.003 ISSN 0022-407

Tousey R, Hulburt EO (1947) Brightness and polarization of the daylight sky at various altitudes above sea level. J Opt Soc Am 37(2):78–92. https://doi.org/10.1364/JOSA.37.000078

Travis LD (1979) Imaging and polarimetry with the pioneer Venus orbiter cloud photopolarimeter. In: SPIE 0183 Space Optics II. https://doi.org/10.1117/12.957426

Tuchin VV (1997) Light scattering study of tissues. Phys Usp 40(5):495–515. https://doi.org/10.3367/UFNr.0167.199705c.0517

Twomey S, Howell HB (1965) The relative merit of white and monochromatic light for the determination of visibility by backscattering measurements. Appl Opt 4(4):501–506. https://doi.org/10.1364/AO.4.000501

Umov N (1912) Eine spektropolariskopische Methode zur Erforschung der Lichtapsorption und der Natur der Farbstoffe. Physikalische Zeitschrift 13:962–971

Upadhyay D, Mondal S, Lacot E, Orlik X (2011) Full analytical solution of adapted polarisation state contrast imaging. Opt Express 19(25):25188–25198. https://doi.org/10.1364/OE.19.025188

Van de Hulst HC (1981) Light scattering by small particles. Dover Publications, New York

Van de Merwe WP, Huffman DR, Bronk BV (1989) Reproducibility and sensitivity of polarized light scattering for identifying bacterial suspension. Appl Opt 28(23):5052–5057. https://doi.org/10.1364/AO.28.005052

Vasilyev OB, Contreras AL, Velazquez AM, Fabi RP, Ivlev LS, Kovalenko AP, Vasilyev AV, Jukov VM, Welch RM (1995) Spectral optical properties of the polluted atmosphere of Mexico City (spring-summer 1992). J Geophys Res 100(D12):26027–26044. https://doi.org/10.1029/95JD02370

Veselovskii I, Kolgotin A, Griaznov V, Müller D, Wandinger U, Whiteman DN (2002) Inversion with regularization for the retrieval of tropospheric aerosol parameters from multiwavelength lidar sounding. Appl Opt 41(18):3685–3699. https://doi.org/10.1364/AO.41.003685

Veselovskii I, Kolgotin A, Müller D, Whiteman DN (2005) Information content of multiwavelength lidar data with respect to microphysical particle properties derived from eigenvalue analysis. Appl Opt 44(25):5292–5303. https://doi.org/10.1364/AO.44.005292

Wang Y, Hu B, Le HQ (2007) Laser Multi-Spectral Polarimetric Diffuse-Scatter Imaging. In: Proceeding SPIE 6565, algorithms and technologies for multispectral, hyperspectral, and ultraspectral imagery XIII, 65650R. https://doi.org/10.1117/12.719247

Ward G, Cushing KM, McPeters RD, Green AES (1973) Atmospheric aerosol index of refraction and size-altitude distribution from bistatic laser scattering and solar aureole measurements. Appl Opt 12(11):2585–2592. https://doi.org/10.1364/AO.12.002585

Weiss-Wrana K (1983) Optical properties of interplanetary dust: Comparison with light scattering by larger meteoritic and terrestrial grains. Astron Astrophys 126(2):240–250 ISSN 0004-6361

Whitehead VS, Coulson K (1990) The space shuttle as a polarization observation platform. In: Proceeding SPIE 1166, polarization considerations for optical systems II, vol 42. https://doi.org/10.1117/12.962877

Wiegner M, Gasteiger J, Kandler K, Weinzierl B, Rasp K (2009) Numerical simulations of optical properties of Saharan dust aerosols with special emphasis on the linear depolarization ratio. Tellus B 61B(1):180–194. https://doi.org/10.1111/j.1600-0889.2008.00381.x

Winker DM, Pelon JR, McCormick MP (2003) The CALIPSO mission: spaceborne lidar for observation of aerosols and clouds. *In:* Proceeding SPIE 4893, lidar remote sensing for industry and environment monitoring III, vol 1. https://doi.org/10.1117/12.466539

Wolff M (1975) Polarization of light reflected from rough planetary surface. Appl Opt 14(6):1395–1405. https://doi.org/10.1364/AO.14.001395

Wolstencroft RD (1974) The circular polarization of light reflected from certain optically active surfaces. In: Gehrels T (eds) Planets, stars, and nebulae: Studied with photopolarimetry, IAU Coll., vol 23, p 495

Wood SA (1984) Identification of aerosol composition from multi-wavelength lidar measurements. Old Dominion Univ., Dept. of Geophysical Sciences, Norfolk, VA, United States, NASA-CR-173445, NAS 1.26:173445, GSTR-84-4

Yamamoto G, Tanaka M (1969) Determination of aerosol size distribution from spectral attenuation measurements. Appl Opt 8(2):447–453. https://doi.org/10.1364/AO.8.000447

Yang P, Liou KN (1996) Finite difference time domain method for light scattering by small ice crystals in three-dimensional shape. J Opt Soc Am A 13:2072–2085. https://doi.org/10.1364/JOSAA.13.002072

Yang X, Wenig M (2009) Study of columnar aerosol size distribution in Hong Kong. Atmos Chem Phys 9:6175–6189. https://doi.org/10.5194/acp-9-6175-2009

Yang P, Liou KN, Mishchenko MI, Gao B-C (2000) Efficient finite-difference time-domain scheme for light scattering by dielectric particles: application to aerosols. Appl Opt 39:3727–3737. https://doi.org/10.1364/AO.39.003727

Yang P, Feng Q, Hong G, Kattawar GW, Wiscombe WJ, Mishchenko MI, Dubovik O, Laszlo I, Sokolik IN (2007) Modeling of the scattering and radiative properties of nonspherical dust-like aerosols. J Aerosol Sci 38(10):995. https://doi.org/10.1016/j.jaerosci.2007.07.001

Yee SK (1966) Numerical solution of initial boundary value problems involving Maxwell's equation in isotropic media. IEEE Trans Antennas Propag AP-14:302–307. doi:10.1.1.172.6957.

Yi B, Hsu CN, Yang P, Tsay SC (2011) Radiative transfer simulation of dust-like aerosols: Uncertainties from particle shape and refractive index. J Aerosol Sci 42(10):631–644. https://doi.org/10.1016/j.jaerosci.2011.06.008

Yoshiyama H, Ohi A, Ohta K (1996) Derivation of the aerosol size distribution from a bistatic system of a multiwavelength laser with the singular value decomposition method. Appl Opt 35 (15):2642–2648. https://doi.org/10.1364/AO.35.002642

Young AT (1981) Rayleigh scattering. Appl Opt 20(4):533. https://doi.org/10.1364/AO.20.000533

Yurkin MA, Hoekstra AG (2007) The discrete dipole approximation: an overview and recent developments. J Quant Spectrosc Radiat Transfer 106(1–3):558–589. https://doi.org/10.1016/j.jqsrt.2007.01.034

Zakian C, Pretty I, Ellwood R (2009) Near-infrared hyperspectral imaging of teeth for dental caries detection. J Biomed Opt 14(14):64047

Zeylikovich I, Kartazaev V, Alfano RR (2005) Spectral, temporal, and coherence properties of supercontinuum generation in microstructure fiber. J Opt Soc Am B 22:1453–1460

Zhang H, Voss KJ (2009) Bidirectional reflectance and polarization measurements on packed surfaces of benthic sediments and spherical particles. Opt Express 17(7):5217–5231. https://doi.org/10.1364/OE.17.005217

Zhao F, Gong Z, Hu H, Tanaka M, Hayasaka T (1997) Simultaneous determination of the aerosol complex index of refraction and size distribution from scattering measurements of polarized light. Appl Opt 36(30):7992–8001. https://doi.org/10.1364/AO.36.007992

Zhao W, Xu X, Dong M, Chen W, Gu X, Hu C, Huang Y, Gao X, Huang W, Zhang W (2014) Development of a cavity-enhanced aerosol albedometer. Atmos Meas Tech 7:2551–2566. https://doi.org/10.5194/amt-7-2551-2014

Zieger P, Ruhtz T, Preusker R, Fischer J (2007) Dual-aureole and sun spectrometer system for airborne measurements of aerosol optical properties. Appl Opt 46(35):8542–8552. https://doi.org/10.1364/AO.46.008542

Zimnyakov DA, Sinichkin YP, Tuchin VV (2005) Polarization reflectance spectroscopy of biological tissues: diagnostic applications. Izv Vyash Uchebn Zaved Radiofiz 47:957–975

http://www.springer.com/978-3-319-70807-2

Springer Series in Light Scattering
Volume 2: Light Scattering, Radiative Transfer and
Remote Sensing
Kokhanovsky, A. (Ed.)
2018, VII, 299 p. 75 illus., 33 illus. in color., Hardcover
ISBN: 978-3-319-70807-2